LA-6530-PR
Progress Report

UC-15
Issued: October 1976

Nuclear Safeguards Research

Program Status Report

January—April 1976

Nuclear Safeguards Research Group, R-1
Nuclear Safeguards, Reactor Safety and Technology Division

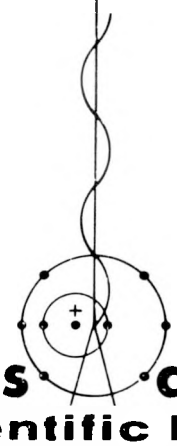

los alamos
scientific laboratory
of the University of California
LOS ALAMOS, NEW MEXICO 87545

UNITED STATES
ENERGY RESEARCH AND DEVELOPMENT ADMINISTRATION
CONTRACT W-7405-ENG. 36

The four most recent reports in this series, unclassified, are LA-5889-PR, LA-6040-PR, LA-6142-PR, and LA-6316-PR.

This work was supported by the Division of Safeguards and Security, US Energy Research and Development Administration.

Printed in the United States of America. Available from
National Technical Information Service
U.S. Department of Commerce
5285 Port Royal Road
Springfield, VA 22161
Price: Printed Copy $4.00 Microfiche $2.25

ABSTRACT

This report presents the status of the two Nondestructive Assay Research and Development programs pursued by the LASL Nuclear Safeguards Research Group R-1 during the period January-April 1976. Salient topics of the two programs are summarized in the table of contents.

CONTENTS

PART I
NUCLEAR MATERIAL SAFEGUARDS PROGRAM— NONDESTRUCTIVE ASSAY TECHNIQUES

I. NONDESTRUCTIVE ASSAY APPLICATIONS AND RESULTS

A. Holdup Measurements at the Kerr-McGee Plutonium Facility (J. W. Tape, M. L. Evans, N. Ensslin, and R. Siebelist)

An independent verification of the plutonium holdup at the Kerr-McGee Nuclear Plutonium Facility took place in February (see Ref. 1, Sec. I-A, p. 1). The US Energy Research and Development Administration (ERDA) sent a team consisting of four members from the Technical Support Organization at Brookhaven National Laboratory, four members from the Los Alamos Scientific Laboratory (LASL) Group R-1, and a representative from ERDA's Division of Safeguards and Security (DSS) to measure holdup in the plant during the weeks of February 9 and February 23. The data were analyzed between the two visits and for approximately 3 weeks afterwards. A report to the Nuclear Regulatory Commission (NRC) is in preparation and will be issued through the DSS.

Most of the measurements were made with NaI(Tl) detectors and stabilized assay meter (SAM) electronics. The SNAP II neutron detector (Ref. 1, Sec. II-B, pp. 5-6) was used in a number of instances when severe gamma-ray attenuation was expected. Neutron-based assay with a directional detector such as the SNAP II was a valuable addition to holdup measuring techniques. However, high backgrounds and room scattering made SNAP II usage difficult. The experimental use of a sensitive, large-area neutron detector to measure the room neutron level was successful within the rather large errors encountered in holdup measurements (see Sec. I-B).

The measurement program at Kerr-McGee provided valuable experience in dealing with holdup problems. The approximately 50% error in the final holdup value resulted primarily from uncertainties of a geometrical nature, i.e., where the source is located. Future plant construction can eliminate many of these uncertainties with equipment designed for minimal holdup and for ease of nondestructive assay (NDA) measurement. Calibration measurements taken in a clean plant before startup will also eliminate many of the problems encountered at Kerr-McGee. A real-time measurement system based on well-defined material balance areas (MBAs) can help reduce holdup uncertainties by providing information about the buildup of material as a function of time. Holdup that does occur will be in a well-defined location and should be relatively easy to measure.

B. Total Room Holdup of Plutonium Measured with a Large-Area Neutron Detector (J. W. Tape, D. A. Close, and R. B. Walton)

The determination of the quantity of plutonium remaining in and on process equipment in large facilities after an inventory cleanout is generally a difficult and time-consuming task involving multiple measurements with portable neutron and gamma-ray NDA devices. For a variety of reasons, the uncertainties associated with such holdup measurements tend to be large and are not easily improved in an existing plant. To reduce the time and effort expended in measurements that generally achieve only a 50% accuracy, LASL began experiments to explore the possibility of determining the plutonium holdup in a room by making a few measurements with a large-area neutron detector.

The principle underlying this technique is that in an isolated room with source material spread uniformly over a plane near the floor, the radiation flux at the center of the room is proportional to the amount of source material present. Such a situation is approximated in a facility after a cleanout when most of the holdup plutonium is on glovebox surfaces and equipment. Neutron detection has a number of advantages over gamma-ray detection in this application; shielding is usually not a major problem, and neutrons scattered from the room surfaces (room return) tend to increase the detector sensitivity to material near the edges of the room.

A large-area neutron detector has been constructed consisting of five 2.54-cm-diam by 50.8-cm active length ^{3}He tubes (4 atm pressure) embedded in a polyethylene moderator 10.2 cm deep, 64.7 cm high, and 35.6 cm wide. The five tubes are connected in parallel to an Eberline* SAM that provides the high-voltage supply and the signal processing electronics. Cadmium absorbers have been eliminated from the detector faces to obtain sensitivity to scattered neutrons of low energy.

The detector has been used both in laboratory situations and in a large plutonium facility. The measurement technique consists of suspending the slab-shaped detector from the center of the room and counting for a period of time such that the statistical error of the measurements is less than 10%. Raising the slab off the floor decreases the sensitivity to local minor variations in the source distribution and generally reduces the shielding effect from objects on the floor. In a situation where material uniformity is unknown, placing the detector at more than one point in the room can provide an indication of the source distribution. A nonuniform source will increase the uncertainties associated with the measurement by an amount that depends on the location and strength of the hot spot.

The detector response to a source of known strength can be expressed as

$$R = N_g \cdot S \cdot \epsilon \cdot A \cdot \phi,$$

where R is in counts/min, N_g is in grams of plutonium, S is the number of neutrons emitted per gram of plutonium per minute, ϵ is the probability that a neutron incident on the detector will be counted, A is the area of the detector faces, and ϕ is the number of neutrons/cm^2 at the detector position per source neutron emitted.

To measure the holdup for a given room, R must be determined by counting for a fixed time and then correcting for any background contribution. Background counts can result from cosmic-ray interactions in the detector, electronic noise, and neutrons from adjacent rooms. If the rooms are well shielded from one another and the room in question contains a reasonable amount of material, background contributions can probably be neglected. In any real situation, the background is difficult to measure directly, as it would require counting in the room with no nuclear material present. Counting in a clean room far from any nuclear material will determine the cosmic-ray and electronic noise contribution; counting in a clean room adjacent to a room containing nuclear material will provide an indication of the wall penetration background.

Once the detector response R has been measured, N_g can be calculated if the other parameters are known. The neutron source strength S is frequently not well known and can change dramatically throughout a facility because of (α,n) reactions with low Z elements that may be involved in the chemical processing. For example, a gram of $^{240}PuO_2$ emits 170 n/s, whereas a gram of $^{240}PuF_4$ emits 1.6(10)^4 n/s.[2] Uncertainties in S are likely to be the largest source of error in this type of measurement. Standards that are representative of the material encountered in each room can be used to determine S and reduce the errors. Note that errors from the increase in (α,n) rates from low Z elements will always increase the measured holdup.

Of the remaining three parameters, A and ϵ concern the detector and ϕ depends on room size and construction, source distribution, and objects in the room. The best way to determine the product $\epsilon \cdot A \cdot \phi$, and hence calibrate the detector-room combination, is to move a known point source around the room in a closely spaced uniform grid pattern to simulate a uniform source distribution. The total response from source placement (corrected for background from material present in the room and from other sources) and the known total number of neutrons emitted allow $\epsilon \cdot A \cdot \phi$ to be determined for that particular room. If the grid placement of the point source is

---

**Eberline Instrument Corporation, Santa Fe, NM 87501.*

representative of the actual material distribution, the calibration will be quite accurate. This procedure also indicates the detector sensitivity to local hot spots.

When calibration with a known source cannot be accomplished, the detector efficiency ϵ and the neutron flux ϕ must be determined by other means. The five-tube ^{3}He slab detector efficiency was measured at 0.5 MeV using an AmLi source of known intensity. Neutrons produced using the ^{7}Li(p,n)^{7}Be reaction from a Van de Graaff accelerator were used to establish the energy dependence of ϵ for $0.065\ \text{MeV} \leq E_n \leq 1.5\ \text{MeV}$. The experimental data are shown in Fig. 1 along with the results of a detailed Monte Carlo model calculation of the detector efficiency from 1 eV to 10 MeV. Both the experiment and the calculation show that ϵ is constant as a function of energy for $1.0\ \text{eV} \leq E_n \leq 0.5$ MeV. For a room-scattered fission spectrum, an ϵ of 12% is reasonable. (The 10% relative uncertainty in ϵ is small compared to other errors encountered in the calibration procedure.)

The calculation of ϕ, the number of neutrons/cm^2 at the detector position per source neutron emitted, is a difficult exercise involving the use of Monte Carlo computer codes. A simplified model of the detector-room combination must be used for the computation to be completed in a limited amount of time. Thus, large errors can enter into this procedure, for example, from objects in a room which are not included in the model.

To test the accuracy of a calculation of ϕ, experimental data were obtained by suspending the detector in the center of an empty, well-shielded room and placing a neutron source on a grid pattern in the room. The 30 source positions on the grid produced an average count rate of 9100 counts/min per point. The rate varied from a maximum of 11 400 counts/min to a minimum of 7100 counts/min with a calculated standard deviation of 1100 counts/min. The room dimensions and construction (a clean hot cell 10 m long, 3.2 m wide, 5 m high with a 0.64-cm-thick stainless steel liner over thick concrete walls) were input to a program that calculated $A \cdot \phi$, the number of neutrons incident on an elliptic cylindrical detector (of dimensions similar to the slab-shaped detector) per incident source neutron. This model detector shape saved computer time. The measured and calculated rates are shown in Table I for various source positions and for an area source. The calculated counts/min were obtained from the computed value of ϕ, the measured ϵ, the known value of S, and the detector area A. The computed rates are the result of a weighted average of two independent 5-min runs on a CDC 7600. There is reasonable agreement between experiment and calculation within the rather large errors in the computed values. (The stainless steel liner and thick

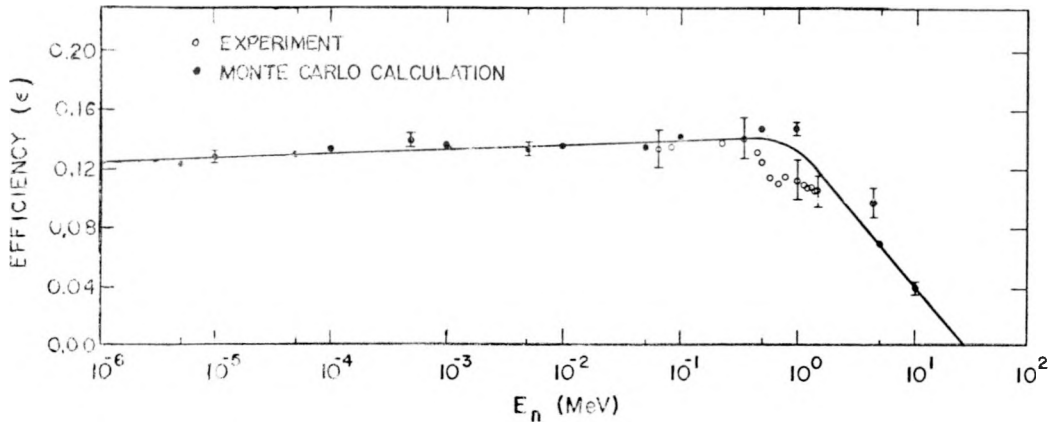

Fig. 1.
Comparison of experimental and calculated efficiency for the large-area neutron detector. The connecting line serves only to guide the eye.

TABLE I

EXPERIMENTAL VERSUS CALCULATED COUNT RATES IN A SMALL ROOM

Source Position (cm)[a]	Experimental Counts/min	Calculated Counts/min
25	8 050 ± 100	10 500 ± 4 000
125	9 240 ± 100	18 500 ± 6 000
225	10 100 ± 100	17 000 ± 5 000
550	7 000 ± 100	6 000 ± 3 000
Uniform floor distribution	8 000 ± 100	13 000 ± 4 500

[a]Horizontal distance from the detector position to a $3.4(10)^7$ n/min AmLi source.

concrete walls require long computing times to obtain good Monte Carlo statistics.) These results indicate that under favorable circumstances, a room holdup value can be obtained without using an empirical calibration to an accuracy of approximately 50%.

To date, field experience with the detector has been limited to a measurement of the plutonium holdup in six rooms of the process area of a facility manufacturing mixed uranium-plutonium oxide fuel pellets. The plant was well configured for a measurement of this type in that the only material present in each room was holdup material, and the rooms were well shielded from one another. The measurement procedure described above was used to obtain counting data for each room. The variation of count rate for different detector positions within each room was less than 15%, indicating that there were no large accumulations of material in a single location.

Empirical calibration with a source was not possible, therefore Monte Carlo calculations previously described were employed to determine the flux ϕ for each room. Room dimensions and wall construction were input to the program which assumed that a uniform source of 2-MeV neutrons was distributed near the floor (the calculated flux was found to be insensitive to initial neutron energy). The computation did not allow for the possible effects of a vertical distribution of source material or for equipment present in the room.

TABLE II

HOLDUP MEASUREMENT COMPARISON BETWEEN LARGE-AREA NEUTRON DETECTOR AND NaI(Tl) GAMMA-RAY DETECTOR

	Relative Holdup Value		
Room	Case 1	Case 2	γ
1	0.31	0.31	0.22
2	0.27	0.21	0.21
3	0.24	0.19	0.16
4	0.32	0.26	0.15
5	0.13	0.11	0.14
6	0.24	0.19	0.12
Total[a]	1.51	1.27	1.00

[a]All values ± 50%.

Results for the six rooms of the plant are shown in Table II along with holdup values obtained using more time-consuming gamma-ray measurements. All quantities have been normalized to the total holdup measured with the gamma-ray technique. Two different values of the specific activity were assumed, and gram quantities were obtained using the calculated value of ϕ and the other known quantities (ϵ, A, R).

The specific activity of the material was known reasonably well only in Room 1; in the other rooms there was a possibility of a large (α,n) contribution to the neutron source strength. In Case 1 the specific activity used for all rooms was calculated for the well-characterized dry material found in Room 1. Rooms 2-6 were wet process areas; it is probable that the material there emitted more neutrons/g-min than the dry source. For Case 2, a wet area specific activity for Rooms 2-6 was obtained by using the gamma-ray measured holdup in Room 2 as a calibration. The dry area source strength was again used for Room 1.

There is good agreement between the large-area neutron detector and the gamma-ray detector holdup measurements. Note that both sets of measurements have approximately 50% uncertain-

ties associated with them. The gamma-ray-based determination required 10 days of effort by two measurement teams whereas the neutron counting was completed in less than 1 day by a single team.

Measurement of plutonium holdup with a large-area neutron detector can be as accurate as NaI(Tl)-based gamma-ray measurements if the requirements of material uniformity and room-to-room shielding are fulfilled, and if the specific activity of the material is known. Room calibration with a known source is preferable to Monte Carlo calculations. However, when unavoidable, the computational technique will work. In situations where the material is nonuniform or shielding is inadequate, the neutron detector might still be used to assure that no large lumps of material were missed by other types of holdup measuring techniques.

C. Assay of Uranium-Thorium Mixtures with the Van de Graaff Small-Sample Assay Station (M. S. Krick and H. O. Menlove)

Phase II results[3] of the high-temperature gas-cooled reactor (HTGR) interlaboratory comparison program (Ref. 4, Sec. I-B, p. 2) indicated a small bias in the assays performed by the Van de Graaff small-sample assay station (SSAS).[5] Table III shows the average deviation of the assayed uranium masses to the ERDA-New Brunswick Laboratory (NBL) standard masses for various thorium-uranium ratios. Studies of the thorium effect on uranium assay have been reported previously (Ref. 6, Sec. I-A, p. 1).

TABLE III

HTGR INTERLABORATORY COMPARISON PROGRAM: LASL NDA RELATIVE TO NBL STANDARDS

Nominal Ratio of Thorium to Uranium	Average LASL Deviation Relative to NBL (%)
0	+0.1
10	+0.6
16	+1.0
25	+0.9
Average	+0.65

Further measurements were made with twelve small standard samples of mixed ThO_2 and UO_2, four of which were prepared by LASL Group CMB-1 and eight of which were supplied by ERDA-NBL. Of the NBL samples, six were from the HTGR-Phase II sample set and two (samples A and B) were prepared from the same material used in the Phase II sample set. All samples were in 3-dram glass vials except for A and B, which were in slightly smaller glass vials. Table IV summarizes the contents of the sample vials.

Because the SSAS is sensitive to the samples' hydrogen content,[5] all samples were measured with the LASL hydrogen analyzer (Ref. 1, Sec. II-D, p. 7). The system was calibrated with a 3-dram vial which contained approximately 3 g of water. The results were normalized to 100 for an empty 3-dram vial

TABLE IV

LASL AND NBL SAMPLE DATA

Standards	Number	^{235}U (g)	Nominal Thorium (g)
LASL	51	0.5472	0
	57	0.5559	3
	59	0.5639	9
	60	0.5820	12
NBL: Group 1	A	0.2823	0
	43	0.2866	2.9
	44	0.2878	7.7
	75	0.2888	4.9
NBL: Group 2	B	0.2853	0
	110	0.2914	7.7
	156	0.2823	4.9
	175	0.2887	2.9
LASL[a]	52	0	6
	53	0	12
	54	0	3
	62	1.1264	6

[a]Used in hydrogen analyzer only.

with no cap. Figure 2 shows the results for all samples; error bars indicate counting statistics only. Vials A and B produced high results because their caps (which contain a small polyethylene liner) are not in the same position as those of the other vials. The response to 5 mg of hydrogen is shown near the right edge of the figure. The difference between the average responses of the LASL and NBL standards (excluding A and B) is 0.66 mg of hydrogen. The increase in the response of the SSAS is +0.1%/(mg H);[5] therefore hydrogen content was not a significant contributor to the errors in the uranium-thorium assay.

The twelve samples were grouped into sets with four or five samples per set for assay with the Van de Graaff SSAS. LASL standard 51 was assayed with each set and served as the reference for all measurements. Sets were assayed by counting each sample for 10 min, cycling through the set about five times. This entire counting sequence was then repeated several times. Figure 3 shows the ratio of the assay mass to the standard mass for each series of runs as a function of nominal thorium mass.

The solid line in Fig. 4 is a weighted least squares fit to all the data points in Fig. 3 which correspond to LASL standards; the shaded area is the 67% confidence band. Using LASL standard 51 to normalize the ratios to 1.00000, thorium dependence is given by

$$R(m_{Th}) = 1.00000 + (0.00067 \pm 0.00038)m_{Th},$$

where m_{Th} is the thorium mass in grams and $R(m_{Th})$ is the ratio of assay mass to actual mass before correction for thorium content. The solid points in Fig. 4 are the uncorrected ratios for the assay of all NBL samples; the deltas are the same ratios corrected for thorium content. The 1σ error bars include correction uncertainties for thorium content.

Table V summarizes the average deviations of the assayed masses relative to the standard masses for the NBL samples before and after applying the thorium correction. The average deviation for all NBL samples assayed in this latest experiment is 0.08%.

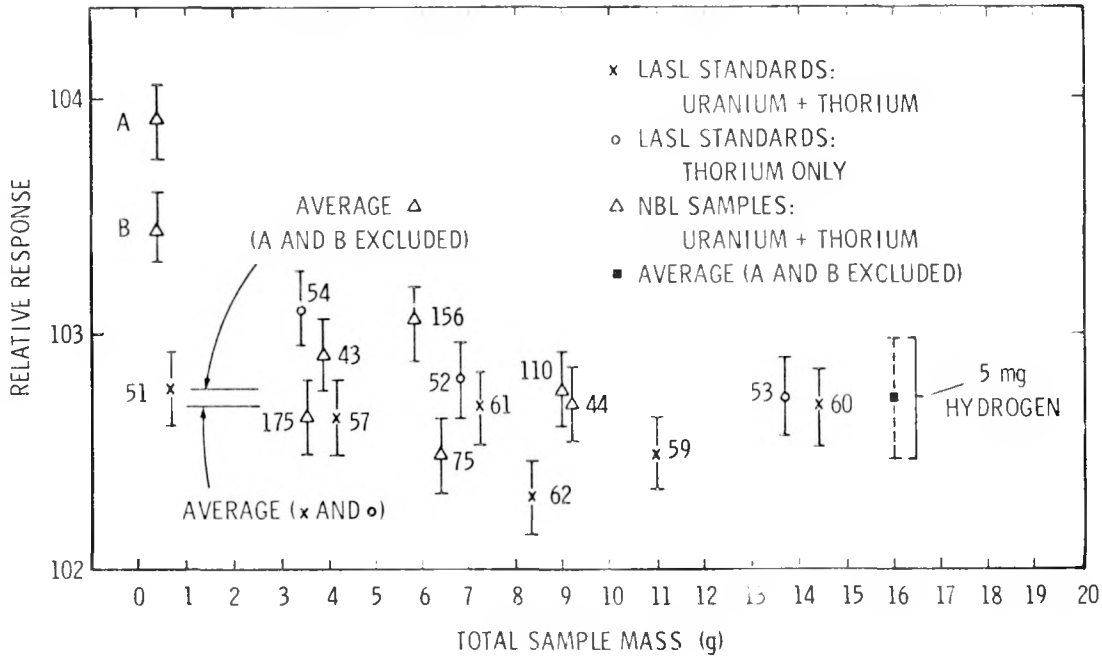

Fig. 2.
Relative response of the hydrogen monitor to uranium-thorium standards. The numbers next to the data points are the sample identification numbers. The response to 5 mg of hydrogen is shown on the right.

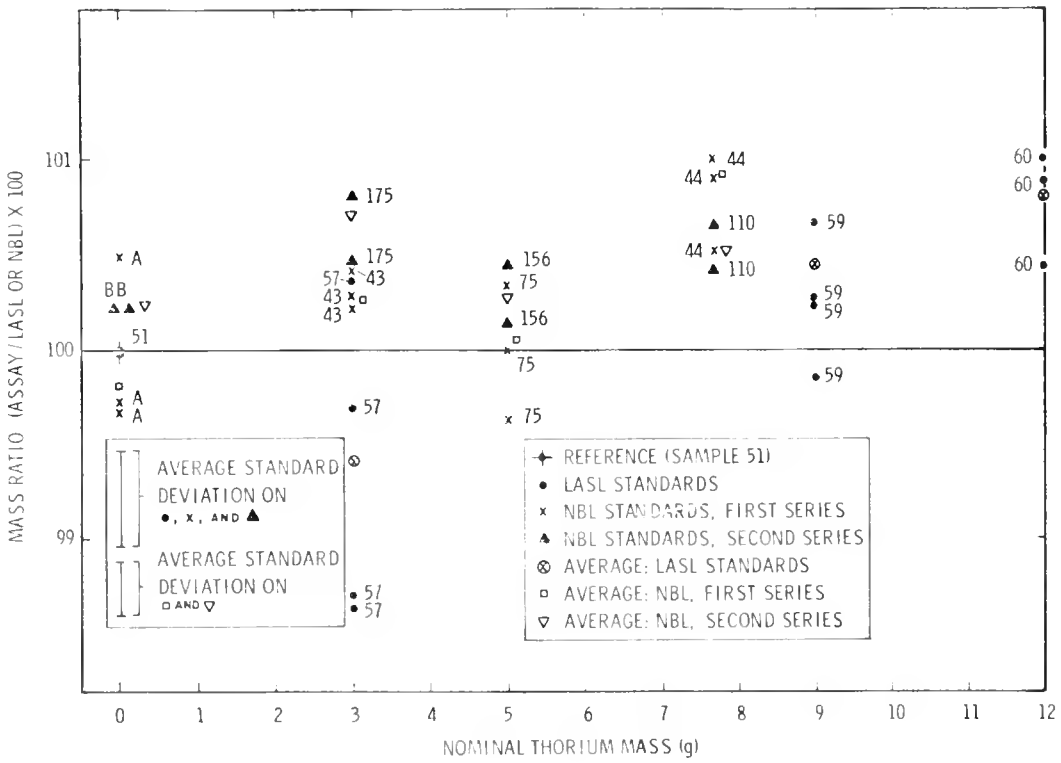

Fig. 3.
Ratio of assay to standard mass (^{235}U) for all series of runs using LASL and NBL uranium-plus-thorium samples. Numbers and letters next to the data points are the sample identification numbers.

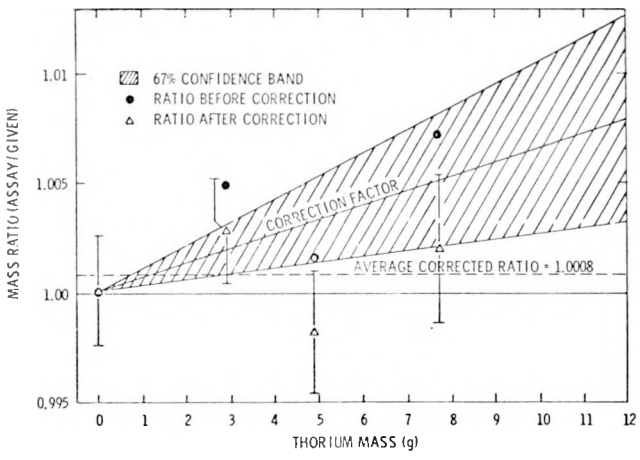

Fig. 4.
Ratio of assay mass to standard mass (^{235}U) for all NBL samples before and after correction for thorium content. The average corrected ratio for all NBL samples is 1.0008.

D. Assay of Low-Level Uranium Samples with the Van de Graaff Small-Sample Assay Station (M. S. Krick)

The super-slab detector (Ref. 7, Sec. I-B, p. 1) was set up in the thermal interrogation mode (Ref. 8, Sec. I-D, p. 10) to assay low-concentration uranium samples by delayed-neutron counting. In addition to placing a polyethylene moderator assembly around the lithium target, the internal sample handling and shielding components of the super-slab were removed to provide space for the assay of large samples.

Natural uranium as U_3O_8 was mixed with damp sand in 7.6-liter polyethylene cylindrical containers (11.3-cm diam by 30.5-cm height). The containers weighed 900 g and the sand weighed approximately 3 kg. Samples were prepared with 0, 1.9, 8.8, 88, and 871 ppm uranium relative to the sand. The counting rate for saturated delayed-neutron activity was

TABLE V

AVERAGE DEVIATIONS OF LASL NDA MASSES RELATIVE TO NBL STANDARD MASSES: PRESENT MEASUREMENTS

Nominal Ratio (Thorium/Uranium)	Average Percent Deviation before Thorium Correction	Average Percent Deviation after Thorium Correction
0	0.0	0.0
10	+0.5	+0.3
16	+0.2	−0.2
25	+0.7	+0.2
Average	+0.35	+0.08

about 0.2 counts/s·ppm and the background was about 0.6 counts/s. The counting rates did not change when the damp sand was replaced with dry sand.

Figure 5 shows the counting time required for assay to 10% (1σ) versus the uranium concentration in ppm. This curve was calculated from measured backgrounds and saturated delayed-neutron counting rates and takes into account the fact that the delayed-neutron activity is not saturated for short assay times.

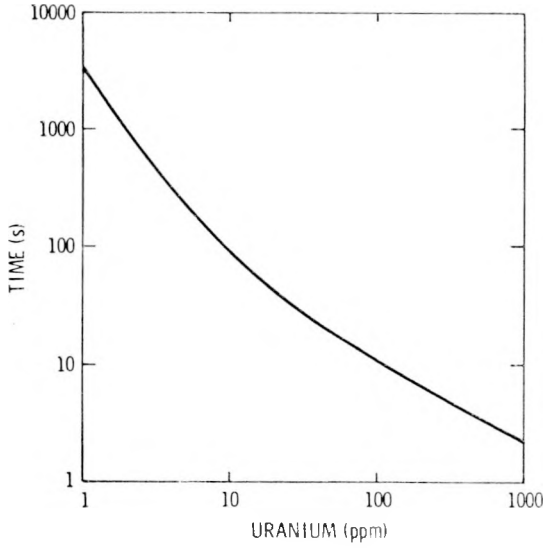

Fig. 5.
Assay time required for 10% (1σ) assay of uranium samples versus the uranium concentration in ppm.

If the sensitivity limit is defined as the net signal being equal to 3σ of the background, then the detection limit is about 4 ppm of natural uranium for a 1000-s measurement time. Because the delayed-neutron response is all from ^{235}U, this sensitivity limit is about 0.03 ppm for 93% enriched ^{235}U. Note that similar sensitivities can be obtained for the assay of solutions containing low concentrations of ^{235}U or plutonium.

E. Measurement of Low-Level Waste (E. R. Martin and T. W. Crane)

The automated box counter used at LASL for waste measurements was removed from the CMB-11 counting room to a new location which has a 30% lower nominal background rate and is not subject to the large fluctuations in background that occur in the counting room when barrels of high-level plutonium-bearing material are introduced. The lower background has greatly improved amplifier stability.

The computer analysis codes were updated in a continuing effort to improve the reliability of the NaI(Tl) system, to incorporate automatic operator diagnostics, and to permit the inclusion of a germanium detector in the system. The changes in the computer code can be introduced without disrupting the routine assay schedule at DP Site. To facilitate

operator use and technology transfer, a manual was published for the box counter system.[9]

A large-area planar intrinsic germanium detector (1000 mm^2 x 12 mm thick) was purchased to supplement the NaI detector now in use. The high resolution of the germanium detector (568 eV at 6.4 keV and 720 eV at 122 keV) can be used to identify the isotopic content of boxes having activity above the 10 nCi/g limit. Measurement of the low-energy efficiency of the germanium detector has shown it to be consistent with expected behavior. Counting rates in the detector positioned 43 cm from an 88-μg plutonium source are approximately 1/s for the 13.6-keV line and 1.6/s for the 17.2-keV line. A 1000-s counting time was used to acquire sufficient statistics from this low-level source. The transmissions for a typical trash box at energies of 13.6, 17.2, and 59.6 keV were measured to be 0.48, 0.68, and 0.87, respectively. These values can vary considerably with the matrix density of individual boxes.

Preliminary investigation was begun for the 4π neutron barrel counter at DP Site as a possible low-level waste measuring instrument for high-density materials where gamma- and x-ray signatures cannot be detected. The addition of a 10-cm lead shield between the sample and the neutron counters could make the device suitable for measuring low levels of plutonium in the presence of hot radioactive wastes generated in spent fuel reprocessing. In either case, the neutron assay is based on coincidence counting from spontaneous fissions (^{240}Pu or ^{242}Pu) or from the total neutron counting rate associated with spontaneous fission and (α,n) reactions.

For the spontaneous fission coincidence measurements, counting rates are low because of the low spontaneous fission activity of 4.1 x 10^2 and 7.7 x 10^2 fissions/s/g for ^{240}Pu and ^{242}Pu, respectively. Hence, a knowledge of competing backgrounds is essential. Backgrounds produced primarily by cosmic-ray showers in a simulated lead or iron liner were measured. The results, expressed as equivalent grams of plutonium (6% ^{240}Pu) per 100 kg of material, are 2.86 $\pm$ 0.04 and 0.53 $\pm$ 0.02 for lead and iron, respectively, at an altitude of 2200 m. Thus, measurements with a sensitivity of about 1 g of plutonium in a 210-liter drum should be possible. At sea level where the cosmic-ray background is a factor of 4 lower than at Los Alamos, the technique should be more sensitive. The addition of cosmic-ray veto counters may also lower this background interference. It may be possible to reduce the amount of lead by developing detectors that are insensitive to high gamma-ray levels.

The measurement of total neutron yield is affected by the chemical composition of the sample as well as by the isotopic composition and backgrounds. Errors with this type of measurement will be biased on the high side. Hence, the total neutron flux measurement may be valuable as a GO/NO GO indicator for disposal.

F. Use of Segmented Gamma Scanner for ^{241}Am Measurement (E. R. Martin and J. L. Parker)

Group CMB-11 had in its possession many canisters reputed to contain ^{241}Am waste, which had been carried on the books for the past year. To clear the books and dispose of those containers which were clean, we undertook to accurately measure the americium content in each container.

To perform the analysis, we used the segmented gamma scanner currently in use for routine plutonium ash measurements, and adapted the procedure to permit americium measurements. The americium waste was in thick stainless steel containers, some wrapped in 3.2 mm of lead, thus the only way to make the measurement was based on the 662-keV gamma line from americium because it has sufficient penetrability to escape from the container. Only ^{75}Se was available for the transmission measurement, but the ratios of the mass attenuation coefficients between 400 keV from ^{75}Se and 662 keV are sufficiently constant to permit 10-20% measurements, the stated goal.

The calibration to relate counts in the 662-keV gamma peak to grams of americium was accomplished by counting a well-known cesium source and calculating the yields from it. A cesium source was used which had an activity of 10.17 μCi on January 1, 1970. This meant that it was 6.403 yr old at the time of calibration. Cesium has a half-life of 29.94 yr, yielding an activity of 8.772 μCi at the time of use. After setting broad enough regions of interest around this cesium peak to include the americium peak which is slightly higher in energy, we made several calibration runs and determined that this amount of cesium, which corresponds to 3.246 x 10^5 total

gammas/s, gave an average of 666 counts/s. Because the branching ratio for the 662-keV gamma energy in cesium is 3.46 x 10^{-6}, the total disintegrations are 1.27 x 10^{11}/s·g, our source corresponded to 3.246/4.39, or 0.739 g of americium. Hence, the calibration factor for measuring americium is 901 corrected counts/g.

An assay was then made of 30 canisters of various sizes which were potentially contaminated with americium. The following results were obtained: 14 canisters contained less than 0.1 g of americium, 6 canisters contained between 0.5 and 2 g, 8 canisters contained between 2 and 10 g, and 2 canisters contained over 10 g. Total americium in all containers was 63 g, compared to the previous, arbitrarily assigned value of 30 g.

II. INSTRUMENT DEVELOPMENT AND MEASUREMENT CONTROLS

A. CMB-8 Material Balance System (T. L. Atwell, N. Ensslin, and H. R. Baxman*)

Several improvements have been made in the software for Group CMB-8's material balance system (described in Ref. 1, Sec. II-A, p. 4). The computer programs for the random driver, uranium solution assay device (USAD), and material accounting were condensed and overlaid. A time-sharing monitor was written for both assay instruments to run simultaneously on one terminal while accounting transactions are being entered on the other. All three programs were provided with additional diagnostics, more compact input formats, and faster terminal printout rates to reduce the time required to operate the system. The results of all assays are now saved on floppy diskettes which make available a large amount of organized data for the study of instrumental biases.

The accounting program has been in use since the January 1976 inventory. About 300 transactions per month are being entered. These cover all aspects of the uranium recovery process within the plant. The program calculates ending balances, material unaccounted for (MUF), and the limit of error of MUF (LEMUF) for all material on a real-time basis. Ending balances can be compared against the printouts of the ADASF** accounting program, which are available twice a month. Up to now there have been no discrepancies.

For each account the program calculates MUF as material in minus material out minus mass of material present. This is equivalent to book inventory minus physical inventory if there is no material in process. Because all material is assayed by the random driver or USAD, measurement errors are available for almost all transactions. These errors are combined in quadrature to determine LEMUF for each material account. This procedure may overestimate LEMUF as some errors are correlated. The calculated LEMUF has been reasonable so far.

Future development of the program will concentrate on improved calculations of MUF and LEMUF. Although the uranium recovery is not carried out by batch process, an attempt will be made to establish MBAs around some parts of the process to improve real-time accountability.

B. IAEA Portable High-Level Neutron Coincidence Counter (M. L. Evans and H. O. Menlove)

Preliminary studies are under way to design a portable thermal neutron coincidence counter for use by the International Atomic Energy Agency (IAEA) to assay high-content plutonium samples. The design includes not only optimization of neutron detection characteristics (e.g., absolute efficiency and die-away time), but also considerations such as weight and size that affect the instrument's portability. Restrictions are placed on the counter's weight and dimensions: when disassembled, its components must fit inside a standard suitcase for hand carrying.

Initially the counter was designed as a square configuration made up of four rectangular slabs each containing four ^{3}He tubes. The slabs could be

---

LASL Group CMB-8.

**Assistant Director for Administration, Source, and Fission Materials.*

arranged to form a square-well counter for the assay of sample cans or, alternatively, two slabs could be used in a sandwich configuration to measure neutrons from small samples or fuel rods. Monte Carlo studies of the square-well counter indicated that acceptable values for detector efficiency and die-away time could be obtained, but only with a penalty of excessive weight. As a result, alternate counter configurations were considered.

The geometry ultimately chosen for the counter is hexagonal as shown in Fig. 6. The width of the well (18-cm minimum) accepts standard-size sample cans (approximately 17 cm in diameter) while minimizing counter dimensions and, hence, weight. The design provides enough space to facilitate placement and removal of sample cans.

Each of the six sections of the hexagonal counter contains four 2.54-cm-diam ^{3}He tubes (pressurized to 4 atm) embedded in polyethylene. For the purpose of the Monte Carlo neutron studies, three polyethylene moderator regions were identified. The first moderator is a mechanically separate block of polyethylene located inside the tube-carrying polyethylene block. On both sides of the first moderator is a 0.4-mm-thick cadmium sheet (see Fig. 6b). The ^{3}He tubes divide the second polyethylene block into two moderator sections, one between the tubes and the wall of polyethylene block facing the inside of the counter (Moderator 2), and one between the tubes and the exterior face of the polyethylene block (Moderator 3).

Monte Carlo studies have been performed in which the thicknesses of the three moderators were varied to determine the dimensions yielding maximized detector efficiency and minimized detector die-away time. For the counter shown in Fig. 6 (with a thickness of 0.7 cm for all three moderators), the Monte Carlo calculation predicts an average absolute detection efficiency of about 6% and a die-away time of about 15 μs. The weight of the counter should be approximately 13 kg excluding ^{3}He tubes, junction boxes, and miscellaneous hardware. This counter is presently being fabricated. On completion, experimental studies will be made of the counter to determine its characteristic efficiency and die-away time. A complete report will be written to describe the counter performance and the Monte Carlo results. Parametric curves will be presented to permit easy design of different counters with specified characteristics such as efficiency, die-away time, and weight.

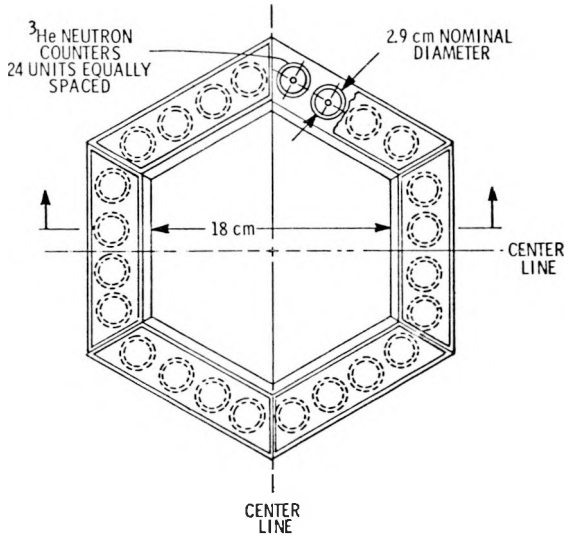

a. Top view.

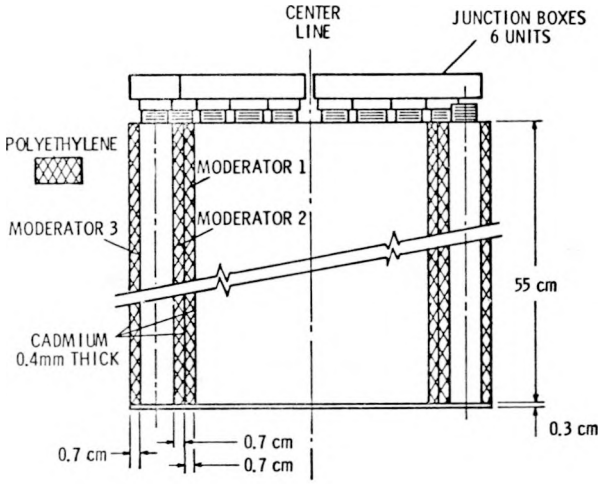

b. Side view.

Fig. 6.
Portable high-level neutron coincidence counter for the assay of plutonium samples in the mass range 100-2000 g.

C. Portable Neutron Assay Systems for Light-Water Reactor Fuel Assemblies (H. O. Menlove, R. Siebelist, M. DeCarolis,* and A. Keddar*)

Development of an NDA method for verification of unirradiated light-water reactor (LWR) fuel assemblies is needed for IAEA inspection purposes.[10] Such confirmation measurements should be capable of determining the ^{235}U content to an accuracy of ±2 to 3% 1σ level. The measurements should also ascertain that no fuel rods have been removed or substituted from the interior of the assembly.

The present investigations (Ref. 11, Sec. III-D, p. 27) are to study neutron assay techniques for boiling water reactor (BWR) and pressurized water reactor (PWR) fuel assemblies. Preliminary measurements have been performed with an AmLi subthreshold neutron source combined with ^4He detectors to count the induced fast neutrons from fission in a BWR element. These measurements indicate that a neutron source strength of about 5 x 10^5 n/s is sufficient and that the detectors have adequate signal-to-background levels. It might be possible to lower the source strength significantly by using more efficient detectors.

The fuel assembly used for the first set of measurements is a 6 by 6 array of BWR rods enriched to 2.34% in ^{235}U. The rods have a fuel length of 1.2 m; it is possible to remove any of them from the array or substitute rods with a 1.77% enrichment. Some initial measurements were performed with the source and detector configuration shown in Fig. 7. For this experimental setup, the net signal rate was 33 s^{-1} using a source strength of 8.6 x 10^5 n/s and 5- by 30-cm ^4He detectors at a pressure of 18 atm. To determine the penetrability of the measurement, fuel rods were removed, one at a time, to be replaced with an empty rod or a steel rod of the same diameter. The measurements gave the same response for steel rod and empty rod substitutions. Figure 8 shows the experimental setup; numbers on the fuel rod positions represent the relative decrease in detector response for 1000-s counts resulting from the removal of a particular rod. It was assumed that the response was the same on both sides of the axis of symmetry. For this experimental configuration the neutron source and detectors were positioned so that the relative response of the different rod locations was uniform, giving good penetration into the interior of this small BWR array. With a 1000-s measurement it was possible to detect the substitution of four 1.77% rods for the normal 2.34% in the center of the assembly. This substitution represents a reduction in the ^{235}U content by 3.5%.

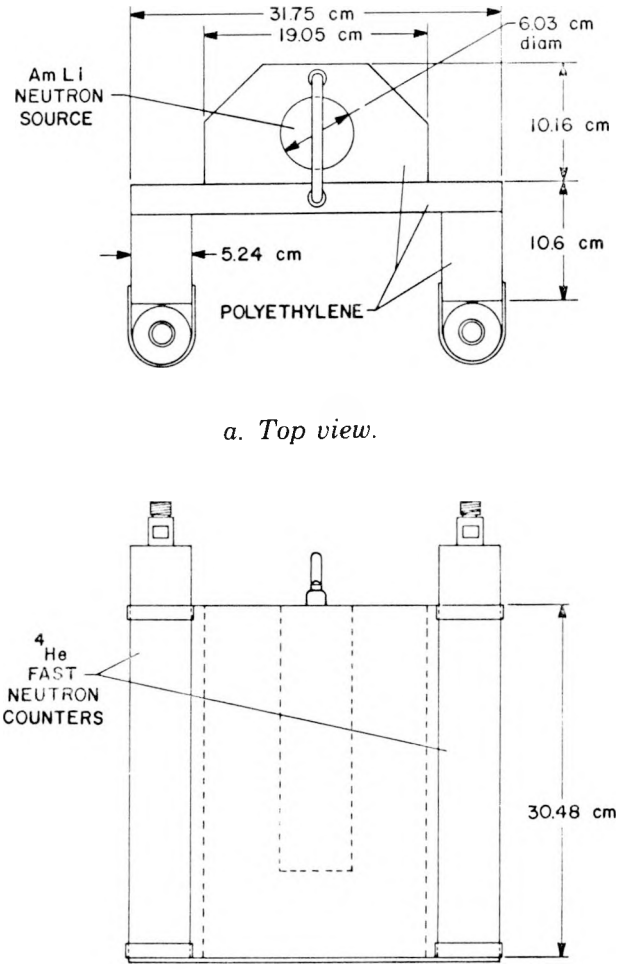

a. Top view.

b. Side view.

Fig. 7.
Portable neutron assay system for LWR fuel assemblies.

Such an interrogation system gives a nonlinear response versus enrichment because of thermal neutron absorption in the ^{235}U. Thus low enrichments give a higher response/gram of ^{235}U than for higher enrichments. It is often the case that fuel

*Staff member of the Department of Safeguards and Inspection, IAEA Headquarters, Vienna.

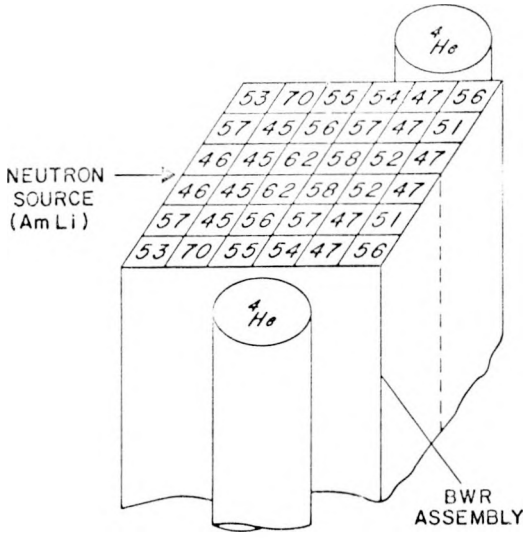

Fig. 8.
Neutron source and detector position for a BWR 6 by 6 fuel rod assembly. The numbers correspond to the relative decrease in counting rate by the removal of the corresponding fuel rod.

assemblies contain more than one enrichment, hence this technique should be used to verify an expected assembly configuration rather than to quantitatively assay an unknown assembly. The presence of burnable neutron poisons in the fuel rods will perturb the results because thermal neutrons are used for the interrogation.

Preliminary measurements of a 15-by 15 rod array PWR assembly (3.12% enriched in ^{235}U) indicate that there is considerably more neutron absorption for the interior rods than for the BWR assembly. To improve the penetration for this larger assembly, the assay configuration shown in Fig. 7 is being modified to improve the neutron penetration for the interior rods.

A prototype assay system of the type shown in Fig. 7 has been loaned to the IAEA for evaluation on its 8-by-8 rod BWR array. This is a short (50-cm-long) assembly containing three different enrichments that can be moved to different positions in the mockup element. The results of these investigations will be reported in the future to help evaluate this assay technique.

D. Neutron Coincidence Correlation Studies (J. E. Swansen, N. Ensslin, and H. O. Menlove)

A method for assay of spontaneous neutron emitters employing a single one-shot time delay has been studied both at LASL and abroad.[1,12] Still unsolved is the problem of a correct separation of neutron detector counts into real and accidental events. This problem has been approached here by attempting to derive a formula for the real counts as a function of detector counts, accidental rate A, one-shot gate lengths τ_1 and τ_2, and detector die-away time τ_D. A derivation from first principles is very involved, but some progress has been made by examining the distribution of time intervals between neutron events.

Figure 9 is a semilog picture of the interval distributions observed with a gate of length τ using a ^{252}Cf source (reals) and an AmLi source (accidentals) counted at the same time inside a neutron well counter. The distribution consists of an accidental term proportional to $\exp[-A(t-\tau)]$ and a real term proportional to $\exp[-(A+1/\tau_D)(t-\tau)]$. This distribution has been studied by varying τ, τ_D, and A, and semiempirical formulas for the real rate have

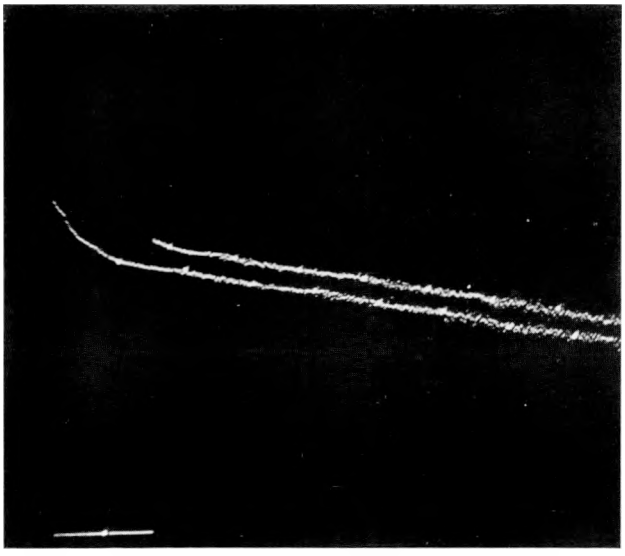

Fig. 9.
Overlapped picture of two interval distributions displayed on a semilogarithmic scale. One distribution is truncated by a 4-μs gate, the other by a 150-μs gate.

been derived. Figure 10 illustrates a recent calculation based on data with $\tau_1 = 4\ \mu s$, $\tau_2 = 150\ \mu s$, and $\tau_D = 31\ \mu s$ (see Ref. 1, Sec. II-F, p. 8 for circuit description). The corrected formula gives an assay that is independent of accidental rate over the range of applicability (≤30 kc) without any free parameters.

More experimental work is required to verify this formula for all cases. The present work does imply, however, that (a) the simple formula is inadequate even at low rates, and (b) assays may be most accurate with one very short gate (τ_1) and one long gate ($\tau_2 \gtrsim \tau_D$) because the separation of reals from accidentals is better in that case.

E. Measurement of the Resolving Time of ^{3}He Proportional Counters (T. L. Atwell)

In the analysis of short die-away time (3-30 μs) neutron coincidence systems that employ ^{3}He proportional counters, the magnitude of the resolving time has been in question. The resolving time is the dispersion in time between ^{3}He(n,p)T interactions occurring at different distances from the anode and the time the event is actually registered as a digital pulse by the electronics. The time dispersion is essentially proportional to the drift velocity or mobility of primary electrons in the gas divided by the radius of the tube. Past measurements of CH_4- and ^{4}He-filled tubes, for example, yielded resolving times of 0.1 μs for a 1.9-cm-diam CH_4 (4.5 atm) tube compared to 17 μs for a 5-cm-diam ^{4}He (18 atm) tube. Consult Ref. 13, Sec. III-E, pp. 12-14 for experimental details.

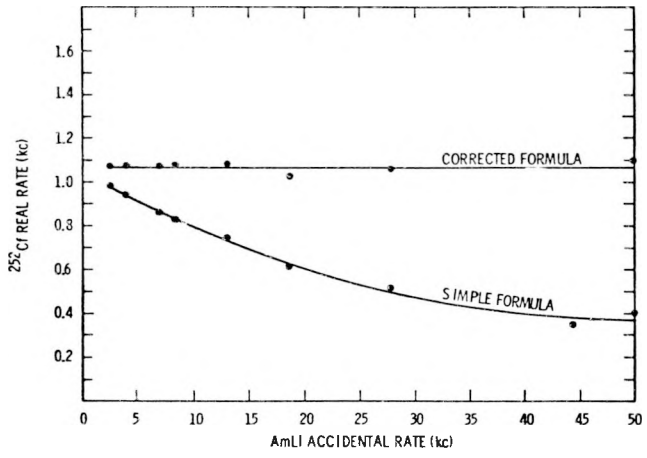

Fig. 10.
Coincidence circuit assay as a function of accidental rate. For the simple formula, see Ref. 1, Sec. II-F, p. 8.

The measurements were made using the setup shown in Ref. 13, Fig. 13. Two 2.5-cm-diam by 51-cm-long ^{3}He-filled (4 atm) proportional counters were tested. One was the standard Reuter Stokes Model RS-P4-0820-203 with stainless steel cathode; the other was a Model RS-P4-0820-103 with aluminum cathode and charcoal liner. The measured time dispersion for each tube was the same, 2.5 μs.

F. Comparison of ^{4}He and CH_4 Proportional Counters for Fast-Neutron Counting (M. S. Krick and H. O. Menlove)

Proportional counters filled with helium and methane were compared with respect to efficiency, gamma-ray insensitivity, temperature stability, and long-term stability. The methane counter was filled to 2 atm and the helium counter was filled to 8 atm to provide the same number of helium or hydrogen atoms per counter. The tubes were 5 cm in diameter by 61 cm in active length. For most measurements the central regions of the tubes were operated in a 5-R/h gamma-ray field produced by a 200-mCi ^{124}Sb-^{60}Co source. Figure 11 shows the pulse-height distributions produced by the ^{4}He counter exposed to a ^{252}Cf source both with and without the 5 R/h gamma-ray background. The corresponding distributions for the methane counter are similar.

Counter efficiencies were measured in the 5-R/h background for various operating voltages and pulse-shaping time constants by integrating the pulse-height distributions above the knee formed by the gamma-ray background. The efficiencies were insensitive to the operating voltages, except for the ^{4}He counter when operated with 0.1-μs time constants. Table VI shows the maximum relative efficiency obtained for each tube with the corresponding operating voltage for various time constants; the integrating and differentiating time constants were equal for all measurements.

The counters were tested for gamma sensitivity by selecting a discrimination level above the gamma-ray pileup and by integrating above this discrimination level for ^{252}Cf spectra obtained with and without the 5-R/h background. Bipolar pulses were used with

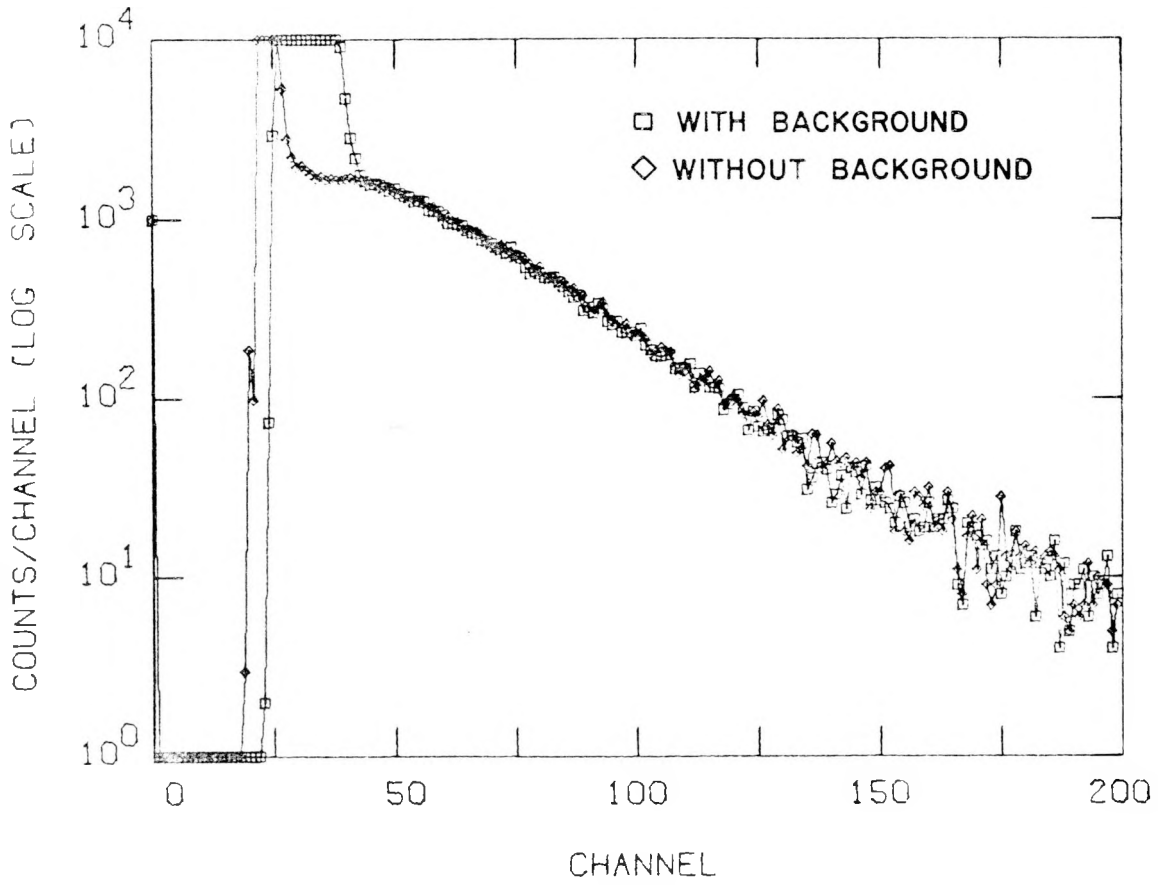

Fig. 11.
Spectrum of ^{252}Cf source taken with an 8-atm ^4He proportional counter with and without a 5-R/h gamma-ray background.

TABLE VI

MAXIMUM RELATIVE EFFICIENCIES OF HELIUM AND METHANE COUNTERS FOR THREE TIME CONSTANTS

	^4He		CH_4	
Time Constant (μs)	**Relative Efficiency**	**High[a] Voltage (V)**	**Relative Efficiency**	**High[a] Voltage (V)**
0.10	88	1600	83	2400
0.25	100	1400	77	1600
0.50	100	1200	62	1600

[a]High voltage producing maximum efficiency for a given time constant.

0.25-μs time constants; the pulse-height analyzer was operated with ac coupling and passive baseline restoration. For both the ^{4}He and CH_4 counters, no statistically significant difference was found in neutron detection efficiency between measurements made with and without the 5-R/h background.

Long-term stability was tested for each counter in a 5-R/h background by counting a ^{252}Cf source for several days in 1000-s increments. The ratio of the experimental-to-theoretical standard deviations for the 1000-s runs was 1.28 (0.55%/0.43%) for the methane tube and 1.38 (0.65%/0.47%) for the helium tube.

Temperature stability was investigated over the range of 40 to 200°C for the ^{4}He and CH_4 counters. The counters were wrapped with heating tape, which was powered by a variable transformer. The counters were surrounded with fiberglass insulation and their temperature monitored with a mercury thermometer. The efficiency of the detectors for counting ^{252}Cf neutrons was measured for approximately 40 temperatures between 40 and 200°C.

The efficiency of the methane counter decreased on an average of 0.04%/°C whereas the efficiency of the helium counter increased on an average of 0.04%/°C.

G. Fast-Neutron Detector Efficiencies (N. Ensslin, T. L. Atwell, M. S. Krick, and J. W. Tape)

For the purpose of neutron detector evaluation, the fast-neutron detection efficiences of a SNAP II detector, a large and a small slab detector, and a Pilot F plastic scintillator have been measured. Plastic scintillator data were needed for studies of matrix effects on the efficiency of random driver instruments (see Ref. 8, Sec. I-C, p. 3 and Ref. 6, Sec. I-D, p. 5). The efficiency of plastic scintillators near threshold is strongly dependent on neutron energy and, in this region, slight shifts in the energy spectrum of prompt fission neutrons caused by matrix materials can change the detection efficiency. Information about the efficiency of the other detectors was useful for the interpretation of recent holdup measurements made with those detectors, and for the characterization of detectors for future applications.

Response as a function of neutron energy over the range 65-1500 keV was measured with the LASL 3.75-MV Van de Graaff accelerator. The response was normalized to a modified long counter[14] to determine the relative efficiency. The intrinsic efficiency was determined by counting neutron sources of known strength.

To confirm that the long counter response was flat as a function of neutron energy, the measured counts were compared to published results for the ^{7}Li(p,n)^{7}Be reaction used to produce the neutrons. Figure 12 illustrates the neutron differential cross section at an angle of 0°, including the contribution of the ^{7}Li(p,n'γ)^{7}Be reaction,[15] against which the present measurements could not discriminate. Compared to this curve are the measured responses of the long counter and a large 51- by 61- by 16-cm-deep polyethylene slab detector containing 13 ^{3}He tubes. These data were corrected for variations in proton beam current and (approximately) for room return background, and then normalized to 152 mb/sr at E_n = 572 keV. Statistical precision is on the order of the size of the data points, but background effects may be larger. Within the accuracy of the measurements, the responses of the long counter and the large slab are found to be flat over the range 65 to 1500 keV.

Figure 13 illustrates the relative efficiency of a SNAP II neutron detector and a smaller 35- by 65- by 10-cm-deep polyethylene slab detector containing five ^{3}He tubes. The SNAP II response was the same with and without extra polyethylene shielding behind the detector. The slab was shielded with cad-

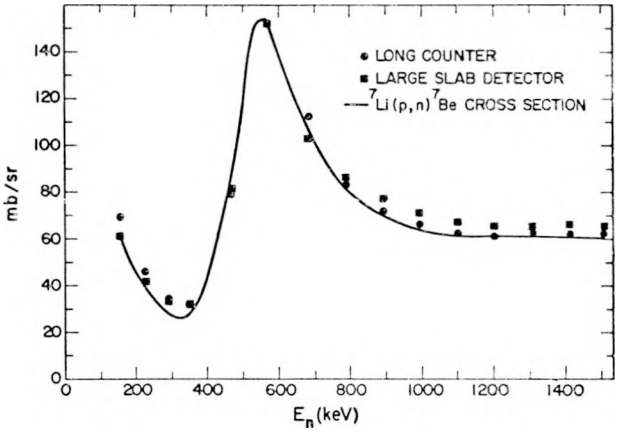

Fig. 12.
Response of long counter and large slab detector.

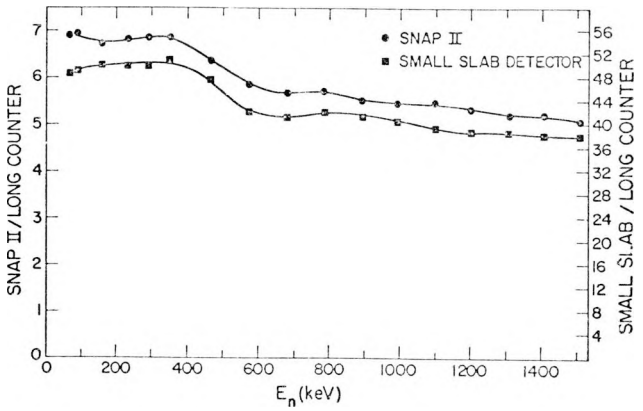

Fig. 13.
Response of SNAP II, small slab relative to long counter.

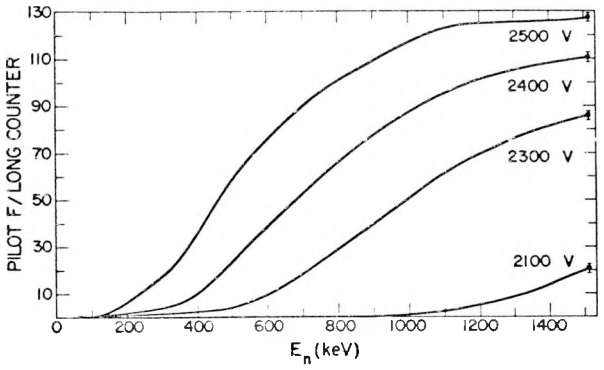

Fig. 14.
Response of Pilot F relative to long counter.

mium and polyethylene on the back face. Both detectors have a smooth response that falls off gradually with increasing neutron energy. For the faster neutrons there is not enough moderating material in these detectors.

Figure 14 illustrates the relative efficiency of Pilot F plastic scintillator for four values of the photomultiplier tube high voltage. The raw data were corrected for a gamma background due to the $^{1}H(n,\gamma)^{2}H$ reaction in the scintillator which occurs as neutrons slow to thermal velocities. This correction was on the order of 10%. For each voltage there is a distinct threshold, and for the higher voltages a plateau is reached. For these measurements the plastic was surrounded by 2.5 cm of lead and 0.6 cm of boral. This amount of lead was the minimum thickness sufficient to remove gamma rays from the beam target and from room background. The boral had only a few percent effect.

Intrinsic efficiencies for these detectors were obtained by counting four known AmLi, one PuLi, and one PuBe sources. (Data concerning the large slab were obtained from Ref. 14.) The results are summarized in Table VII. The long counter was used with only the central ^{3}He tube connected. With all five tubes the intrinsic efficiency is about five times larger.[14] The plastic scintillator was 25- by 61- by 5-cm deep, and was coupled to two RCA 8575 photomultiplier tubes operating at 2400 V. Because the neutron energy spectra of the sources are different, the measured efficiencies vary, particularly for the plastic scintillator.

TABLE VII

INTRINSIC EFFICIENCY OF FAST-NEUTRON DETECTORS

Reference Source	Average Neutron Energy (MeV)	Long Counter (1 tube) (%)	Large Slab[a] (13 tubes) (%)	Small Slab (5 tubes) (%)	SNAP II (2 tubes) (%)	5-cm Pilot 2400 V (%)
AmLi[b] (4)	0.5	2.3±0.1	---	15.0±0.7	18.8±0.8	34±5
PuLi	0.65	2.3±0.1	18.5±0.7	14.3±0.6	17.2±0.7	44±3
PuBe	4.2	1.9±0.1	15.3±0.7	9.6±0.4	12.2±0.5	54±4

[a]See Ref. 14.
[b]See Ref. 15.

H. A Gamma-Ray Perimeter Alarm System (D. A. Close and R. B. Walton)

Several perimeter alarm systems have been considered for monitoring exclusion areas around nuclear facilities. These range from armed guards to more sophisticated systems, such as closed circuit television, infrared monitors, Doppler radar, and electric fences. Each system has inherent disadvantages. The following study of a gamma-ray alarm system was initiated by the suggestion of C. Sonnier from the Sandia Corporation.[16]

A common type of physical protection system is based on the electric-eye principle, where the interruption of a light beam signals the presence of an intruder and activates an alarm. A system based on a light beam has reliability problems because of its sensitivity to weather variations, birds, and leaves. Electromagnetic radiation in the form of gamma rays may be better suited for this application because of the greater penetrability of gamma rays through dense media. The half-thickness for gamma rays in dry air at sea level varies from 37.5 m at 100 keV to 158.0 m at 3000 keV, a range that is sufficiently large to warrant further investigation of the gamma-ray beam interrupt scheme. Electronic systems which detect gamma rays are simple, and none is required at the source of radiation. For these regions, it was suggested that the feasibility of the gamma-ray beam interrupt scheme be seriously considered.[16] Battelle-Columbus Laboratories[17] is currently assessing the use of the particular isotope ^{85}Kr ($t_{1/2}$ = 10.8 yr, $E\gamma$ = 514 keV) for this and other applications.

Initial Monte Carlo gamma-ray transport calculations were performed using the model shown in Fig. 15. Both a single source and a single detector were assumed to be 0.91 m above the ground. The source was located between a concrete wall (simulating the building to be protected) and a fence (simulating an exclusion area) 1.8 m from the wall. Counting rates were calculated assuming a detector placed 93 m from the source for dry and wet soil, for dry and wet air, and with and without the concrete wall present. These different conditions were studied as a function of the gamma-ray energy and only photopeak events were considered.

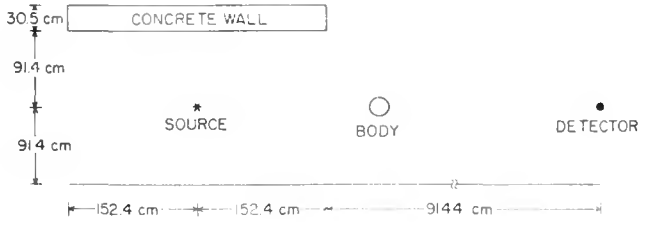

Fig. 15.
Top view of the model used in the Monte Carlo gamma-ray transport calculations.

A possible limiting condition for this system is the attenuation of gamma rays by moisture in the air. For the calculations, a value of 5.0×10^{-5} g/cm^3 for the density of water in the air was assumed. This corresponds roughly to the moisture content of saturated air for an air temperature of 30°C. As will be pointed out later, this is not a critical parameter.

Results of the Monte Carlo calculations showed that the concrete wall had a negligible effect on the predicted count rate. Similarly, the moisture content of the soil did not affect the results. Further calculations thus assumed the wall to be present and the soil to be dry.

The human body was approximated by a water-filled cylinder 15.24 cm in diameter and 122 cm tall. The detector was assumed to be a 12.7- by 12.7-cm NaI with an idealized efficiency of 100% for each gamma-ray energy. A 1-Ci source, 93 m from the detector, was also assumed for the calculations.

The expected count rates as a function of the gamma-ray energy for dry and wet air, with and without a body in the beam, are shown in Fig. 16. The graph spans the energy range of the common radioactive sources applicable to such a system, from the 60-keV gamma ray of ^{241}Am to the 2614-keV gamma ray of the ^{232}Th decay chain.

There is about a 10% difference between the count rates for dry and wet air at 60 keV and a 2% difference at 3000 keV. This change is small, however, compared to the effect of a body. For 60-keV gamma rays, the count rate for the unbroken beam is nine times that for the broken beam. For 3000-keV gamma rays, this factor is 2. In order for wet air to produce a suppression of the count rate comparable to that the body produces, the density of water in the air would have to be about 2.0×10^{-3} g/cm^3, two orders of magnitude larger than the value used. Moist air can thus be eliminated as a possible hindrance to the operation of such a system.

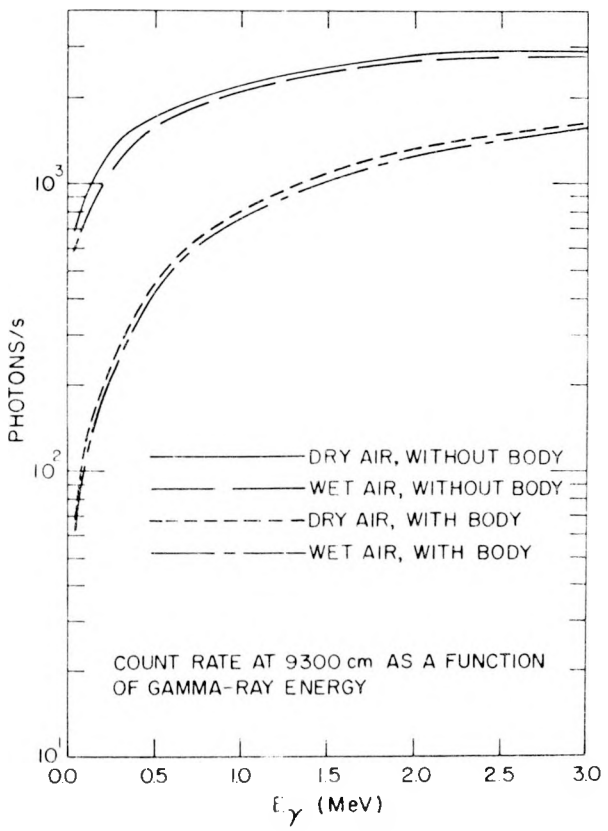

Fig. 16.
Expected count rates for a source-detector distance of 9300 cm as a function of the gamma-ray energy for dry and wet air, and with and without a body breaking the beam. These curves assume a 1-Ci source and a 100% efficient 12.7- by 12.7-cm NaI detector.

This method may be used to determine the number of false alarms expected in a given period of time for the proposed gamma-ray alarm system as a function of the gamma-ray energy. These false alarm calculations are summarized in Table VIII. They are based on the assumption that the intruder will break the beam in 0.05 s. Column 2 lists the count rates for the unbroken beam, and column 3 lists the count rates for the beam broken by a body. The standard deviations of the count rates are taken to be the square root of the count rates. The number of standard deviations the broken beam count rate differs from the unbroken beam count rate is shown in column 4. Column 5 shows the probability that this deviation could occur at random in a 0.05-s time interval. The number of false alarms expected per year, shown in column 6, is calculated by multiplying the probability of a single event happening in a 0.05-s time interval by the number of 0.05-s time intervals in 1 yr. The expected false alarm rate shows a significant minimum around E_γ = 500-1000 keV. (Note that the ^{85}Kr source, E_γ = 514 keV, proposed by Battelle-Columbus Laboratories[17] is an ideal energy source, resulting in a minimum number of false alarms in a 1-yr period.) For lower energy gamma rays, there is significant attenuation of the gamma rays by the air, and for higher energy gamma rays, there is not much attenuation of the gamma rays by the body.

These calculations indicate that a gamma-ray alarm system should be extremely reliable, hence a series of experiments were performed using a 1-Ci ^{137}Cs source. We chose ^{137}Cs because it emits a gamma ray of 662 keV which is in the energy region that produces the minimum number of false alarms as predicted in Table VIII. Furthermore, because ^{137}Cs produces only a single gamma ray, it minimizes any interference from competing gamma rays. The half-life of ^{137}Cs is 30 yr, an advantage in actual applications. From the calculations presented in Table VIII, 1 Ci should protect an interval of 93 m.

The experiment was conducted in a building with a long, narrow high-bay and a source-detector distance of 20.9 m. The high-bay width is comparable to the distance between a fence and a nuclear facility.

A single 12.7- by 12.7-cm NaI detector located 1.2 m above the floor and mounted in a 5.72-cm-thick lead shield was used to detect the gamma rays. The ^{137}Cs source was placed in a cylindrical lead collimator 50.8 cm in length and 10.16 cm in diameter with a 0.714-cm-diam hole along its axis. The signal from the amplifier was fed into a single channel analyzer (SCA) adjusted to detect the 662-keV gamma rays. The output signal from the SCA was, in turn, sent to a multichannel analyzer operated in the multiscaler mode with a dwell time of 0.01 s per channel.

With a source-detector distance of 20.9 m, the radiation level at the detector was less than 0.5 mR/h, presenting a minimal health hazard to personnel. The count rates for four methods of interrupting the beam are shown in Fig. 17. When a person walks through the beam swinging his arms, the count rate is depressed as shown in Fig. 17a, where the effect of the leading arm, the body, and

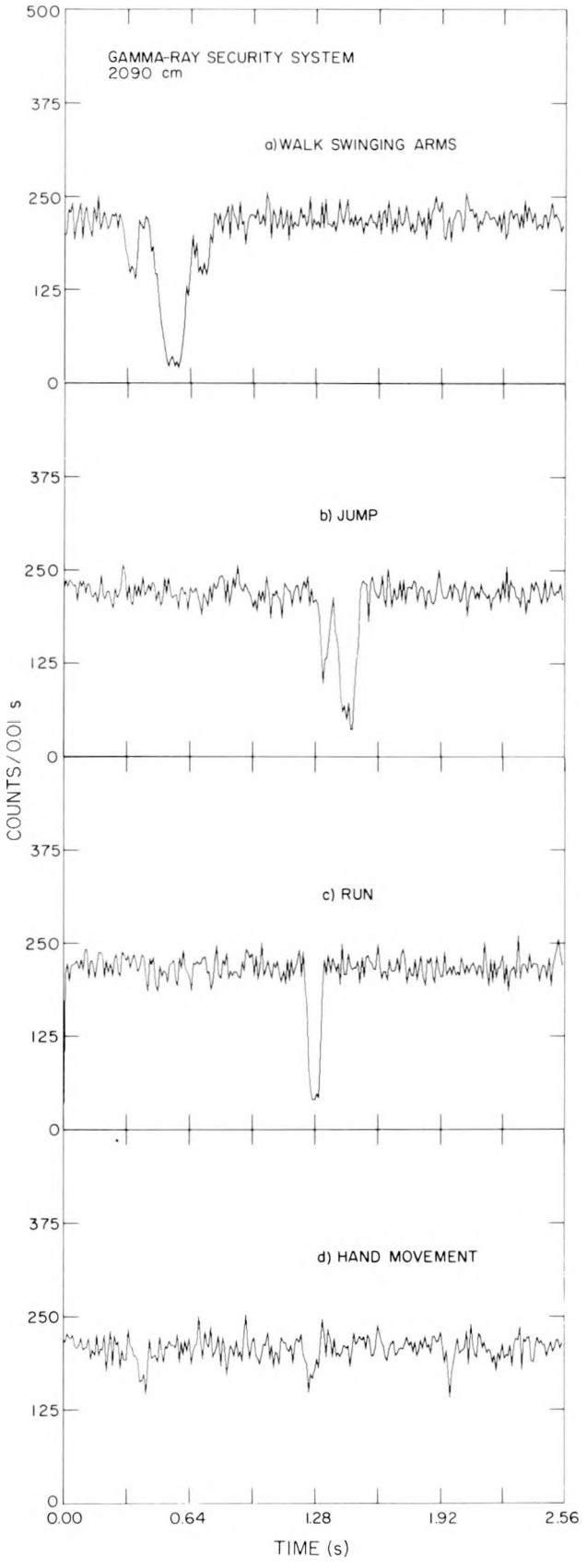

the trailing arm are all clearly seen. Figure 17b shows the situation when a person jumps through the beam; the leading arms break the beam first and then the body follows. The results of running through the beam from a standing start are shown in Fig. 17c. The effect of moving a hand through the beam three times is clearly seen in Fig. 17d.

Table IX summarizes the experimental count rates for various modes of breaking the beam at a source-detector distance of 20.9 m. The standard deviations associated with the count rates are taken to be the square root of the count rates. To run through the beam takes about 0.05 s, thus, this time interval was chosen for the calculations. The table gives the number of false alarms expected in 1 yr. Except for the hand movement case, less than one false alarm per year is calculated with this gamma-ray alarm system.

The proposed gamma-ray perimeter alarm system has been shown to be reliable for detecting intruders. Our results indicate that a much longer source-detector distance can be monitored by a much weaker source than that envisioned by Battelle-Columbus Laboratories.[17] It is an easy task to devise a simple electronic system that will trigger an alarm whenever the count rate varies more than a predetermined amount from the unbroken beam count rate. The electronics should trigger an alarm whenever the instantaneous count rate exceeds the average count rate lest a person try to foil the system by using an additional gamma-ray source.

The next step in developing this concept is to place an actual system in a natural environment to determine the optimum number of sources and the optimum arrangement of detectors.

I. Microprocessors in Nuclear Safeguards Instrumentation (E. R. Martin and D. F. Jones)

Microprocessors were developed primarily for applications where hundreds of identical units are manufactured, thus amortizing development costs

Fig. 17.
Count rates for various ways of breaking the beam with a source-detector distance of 2090 cm: (a) walking, (b) jumping, (c) running, and (d) moving hand.

TABLE VIII

FALSE ALARM PREDICTION FOR GAMMA-RAY BEAMS OF DIFFERENT ENERGIES[a]

E_γ (keV)	Unbroken Beam Counts/ 0.05 s	Broken Beam Counts/ 0.05 s[b]	Number of Standard Deviations[c]	Probability[d]	Number of False Alarms/yr[e]
60	31	3	5.0	4.9×10^{-7}	309
200	55	10	6.1	1.3×10^{-9}	1
500	81	22	6.6	5.0×10^{-11}	<1
1000	106	40	6.4	1.5×10^{-10}	<1
1500	121	54	6.1	1.1×10^{-9}	1
2000	131	65	5.8	7.9×10^{-9}	5
2500	139	75	5.4	5.6×10^{-8}	35
3000	143	81	5.2	2.2×10^{-7}	139

[a]Results of Monte Carlo calculations for a 1-Ci source and a 12.7- by 12.7-cm NaI detector 9300 cm from the source.
[b]Body assumed in the beam.
[c]Number of standard deviations the broken beam count rates are from the unbroken beam count rates.
[d]The chance that this deviation could occur at random in a 0.05-s interval.
[e]The false alarm is the probability multiplied by the number of 0.05-s intervals in 1 yr.

TABLE IX

COUNTING RATES FOR DIFFERENT MODES OF BREAKING BEAM

Mode of Breaking Beam[a]	Unbroken Beam Counts/ 0.05 s	Broken Beam Counts/ 0.05 s	Number of Standard Deviations	Probability	Number of False Alarms/yr
Walk	1093	263	25.2	$<10^{-11}$	<1
Jump	1093	380	21.6	$<10^{-11}$	<1
Run	1093	295	24.2	$<10^{-11}$	<1
Hand Movement	1034	854	5.6	2.1×10^{-8}	13
Arms (walk)[b]	1093	793	9.1	$<10^{-11}$	<1
Arms (jump)[c]	1093	660	13.1	$<10^{-11}$	<1

[a]The source-detector distance was 2090 cm.
[b]Result for arm movement associated with a walk through the beam.
[c]Result for arm movement associated with a jump through the beam.

over long production runs. However, there are many applications in instrument development where only a few of a kind are produced. Some instrumentation for safeguards applications is limited to the few-of-a-kind production level; such instruments involve plant process control and monitor systems and require data acquisition and calculational capability as well as electromechanical control functions. Until recently, these tasks have been relegated to minicomputers supported by a large amount of external hardware. Even in a custom-designed electronics package, the size and complexity provide an impetus to seek a better solution. Our approach has been to replace much of the external hardware with a microprocessor while retaining the minicomputer for complex calculations and data taking. In this way system hardware complexity is replaced by relatively simple microprocessor software, and the minicomputer is retained to perform complex calculations and speed-limited functions.

The 16-bit National PACE microprocessor was selected for linkage to 16-bit minicomputers. It was purchased as a chip set rather than on manufactured boards or as part of a system so that we could better understand the unit and configure it into any physical system. Because our goal was to interface PACE with the minicomputer, we decided to eliminate intermediate steps and go directly into the minicomputer for initial checkout. This eliminated the need to interface a data terminal of any kind or implement a complete front panel. We were also able to try software in random access memory (RAM) before burning programmable read-only memories (PROMs): we loaded test programs directly into RAM via direct memory transfer from the minicomputer at startup. In addition to the direct memory access (DMA) transfer to RAM, we also provided interrupting programmed transfers in both directions between the microprocessor and the minicomputer.

The programming was developed along with the hardware system, beginning with simple machine language instructions loaded into RAM. As the development proceeded, a cross assembler was written to generate code for the PACE on the minicomputer system, which was then loaded directly into the RAM through the DMA as before. The minicomputer also produced a paper tape from which PROMs could later be burned.

Figure 18 shows the overall development system: the 16-bit minicomputer and its terminal together with the microprocessor system and its interface on the cart to the left of the computer. Figure 19 is a closeup of the microprocessor and interface alone, showing the open layout and the simple front panel—two switches and an indicator light-emitting diode (LED)—made possible by the combination of the minicomputer and microprocessor.

Now that this development is complete, we are in a position to provide distributed intelligence for a centralized NDA system whenever needed without long development times, and with a maximum of software development already complete.

J. Segmented Gamma-Scanner Barrel Handler (E. R. Martin and D. F. Jones)

About a year ago, Eberline initiated the manufacture of a mechanical barrel handler which could be added to the existing segmented gamma-scanner to provide 55-gal drum handling capability. The unit was received in late March, and found to fall short of many specifications. To correct these problems, it was necessary to replace the stepper motor, damper, and encoder.

The electronic modifications to permit program switchover between the barrel handler and the small sample table have been designed and are now being implemented in the segmented gamma-scanner system. The new barrel handler should be installed at DP Site within the next few months.

K. Quad Discriminator/Adder for Neutron Array Systems (T. L. Atwell and T. Van Lyssel)

Neutron assay systems using an array of ^3He, BF_3, or ^4He proportional counter tubes in applications where the total count rate exceeds 10 kHz require that the tubes be divided into several groups to minimize the deadtime associated with pulse pileup. Each group of tubes must then have its own preamplifier, amplifier, and discriminator. The individual discriminator outputs must then be ORed together to provide a SUM output to either a scaler or a coincidence module depending on the application.

To complement the commercially available Kicksort 211 Quadamp, we have recently designed

Fig. 18.
Overall microprocessor-minicomputer system.

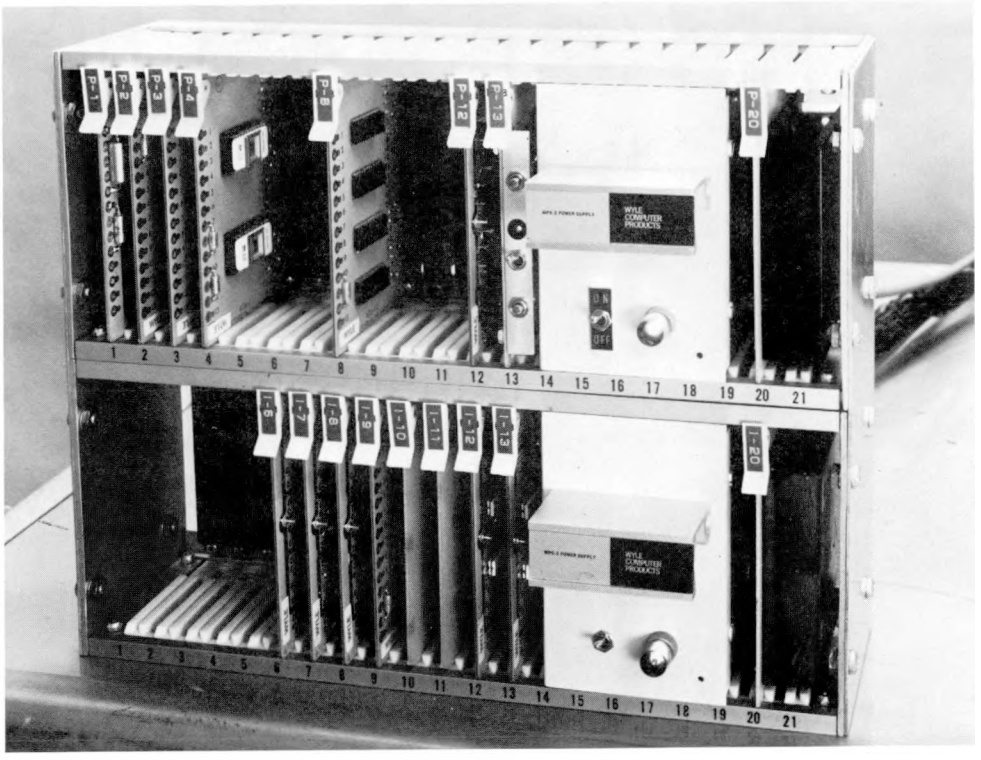

Fig. 19.
Closeup of microprocessor system with its interface.

and built a quad discriminator/adder shown in Fig. 20. This versatile four-channel integral discriminator with ORed outputs is packaged in a single-width, standard nuclear instrument module (NIM). The threshold for each channel can be independently varied over a range from 0.2-10.2 V with an overall linearity of 0.1%. Input pulse hysteresis is internally switch-selectable from 50 to 450 mV for operation in noisy environments. Input impedance is 10 kΩ.

Each of the four discriminator channels can be selectively ORed in several combinations by control switches on the front panel to produce a SUM OUT signal. An external OR input is also provided on the rear panel for the ORing of the SUM outputs of several quad discriminator modules into a TOTAL SUM signal. Furthermore, partial sum outputs are provided on the front panel for discriminator channels 1, 2 and 3, 4 as shown in Fig. 20. The latter feature allows for independent scaling of singles events in different regions of the detector array. This has application where it is necessary to compute front-to-back or inner ring-to-outer ring ratios, for example.

The output drivers produce 100-ns-wide pulses at 5 V into 100 Ω. The pulse pair resolution between channels where outputs are summed is 100 ns.

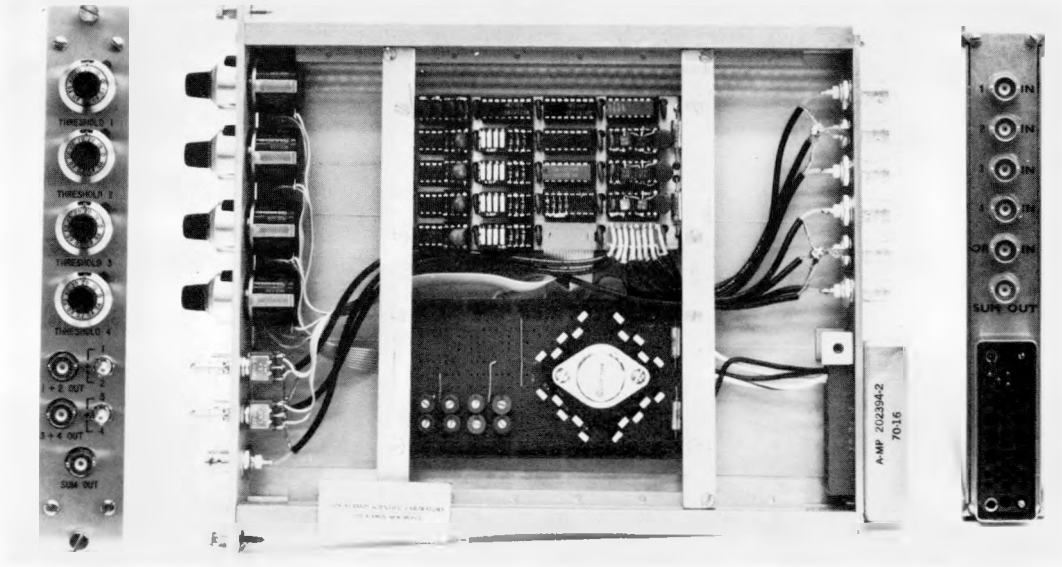

Fig. 20.
Quad discriminator/adder.

PART 2

DEVELOPMENT AND DEMONSTRATION OF DYNAMIC MATERIALS CONTROL—DYMAC PROGRAM

(R-Division, CMB-Division, E-Division Staffs)

Development of the LASL Dynamic Materials Control (DYMAC) program will be presented according to the following format for this and subsequent reports.

Concepts and subsystem development
- NDA instrumentation
- Data acquisition
- Data base management
- Real-time accountability

Implementation and demonstration
- Phase I. Test and evaluation at DP Site
- Phase II. Implementation at new LASL plutonium facility (TA-55)

Technology transfer

Execution of the DYMAC program requires the cooperation of many professional disciplines. Accordingly, during this reporting period particular emphasis was given to assembling an interdisciplinary professional staff in chemistry, chemical engineering, computer science, electrical engineering, nuclear engineering, nuclear materials management, physics, statistics, and technical communications.

I. CONCEPTS AND SUBSYSTEM DEVELOPMENT

A. NDA Instrumentation

Instrumentation Development (T. Gardiner, V. Reams, and M. M. Stephens)

The tasks assigned to the central accounting computer preclude its use for local control of instruments, terminals, and identification equipment. Certain of the nuclear NDA instruments require minicomputers for preliminary data reduction; local control functions can usually be performed using the excess capability of these computers. Some other nuclear NDA instruments do not require dedicated computers: none of the weight measurement or identification units have such requirements. To provide the necessary control functions and to maximize ease of use of the weight measurement and identification units, local microprocessors will be provided. The industry has no clear preference for a particular type of processor or feature, therefore we had to evaluate available hardware and choose a system to satisfy technical and cost objectives. At present we are configuring the Intel 8080 and Motorola 6800 in a variety of ways. As part of this evaluation a microprocessor will control the tests for an evaluation of weighing devices.

Weighing devices of two types will be required for DYMAC: load cells where fair to good accuracy is required, and electronic read-out balances where high accuracy is necessary. A system which will allow repetitive weight measurements on a programmable time scale with a printout of results has been constructed, and testing has been initiated.

DYMAC will employ machine-readable labels for material identification both in storage areas and to identify material in process. A study of material identification systems used in other industrial applications is now in progress. We anticipate that as a result of this study equipment will be procured for trial use at DP Site.

B. Data Acquisition (R. H. Augustson, T. Gardiner, and R. F. Ford*)

A variety of different terminals will be needed to provide the flow of information to and from the production area. These terminals range from a simple set of control buttons to a video terminal with full interactive capability. At present, two types of terminals are being evaluated for use by the process operators. The first provides a hard copy of the information transmitted but it is relatively slow. The second is the simple video terminal which can display data quickly but produces no hard copy. Experience to date suggests that the hard copy terminal is useful for learning the transaction procedure but, for operation, the faster video terminal is preferable.

C. Data Base Management (R.F. Ford*, J. Hagen, and C. Slocomb*)

The commercially available data base management software and hardware is being surveyed in preparation for specifying DYMAC system needs at the new plutonium facility (TA-55). Specifications for the TA-55 computer with software should be ready for bid by the end of the next reporting period.

*LASL Group E-5.

D. Real-Time Accountability

Single-Theft Detection (D. B. Smith)

Consider the detection of a single diversion of special nuclear material (SNM) from a unit process during a given material balance period. We wish to establish criteria for an alarm level (AL) based on the probability densities associated with the measurements used to estimate the material balance, and to determine the concomitant detection probability (DP) and false alarm probability (FAP).

Let the true material balance for the period be denoted by B. If B is greater than zero, diversion has occurred. The true material balance is estimated by the computed material balance b, a linear combination of measurement results. The random variable b is assumed to be distributed normally with mean B and variance σ^2. The relationship between the AL and the true material balance B is shown in Fig. 21. The curve on the left represents the probability distribution of b for the case of no diversion. The other curve is the distribution of b when a diversion of magnitude B has occurred. The shaded areas are DP and FAP as indicated.

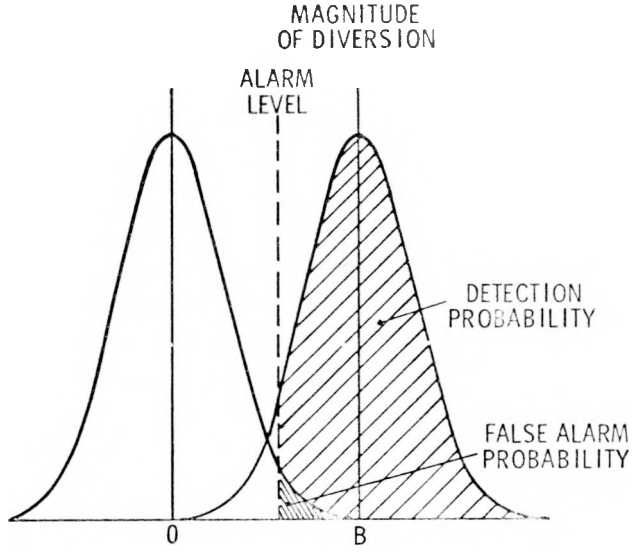

Fig. 21.
Relationship between AL, FAP, and DP for no deviation and for diversion of magnitude B. DP is the sum of the two shaded areas.

DP is given by

$$DP = (\sqrt{2\pi}\,\sigma)^{-1} \int_{AL}^{\infty} \exp\left[-\frac{1}{2}\left(\frac{b - B}{\sigma}\right)^2\right] db \ .$$

FAP is given by

$$FAP = (\sqrt{2\pi}\,\sigma)^{-1} \int_{AL}^{\infty} \exp\left[-\frac{1}{2}\left(\frac{b}{\sigma}\right)^2\right] db \ .$$

By transforming to standard normals we obtain

$$DP = (2\pi)^{-\frac{1}{2}} \int_{(AL-B)/\sigma}^{\infty} \exp\left[-\frac{1}{2} z^2\right] dz \ ,$$

$$FAP = (2\pi)^{-\frac{1}{2}} \int_{AL/\sigma}^{\infty} \exp\left[-\frac{1}{2} z^2\right] dz \ .$$

These expressions are shown in Figs. 22 and 23, and may be considered design curves for the establishment of an AL based on the measurement variance σ^2. If the measured material balance b exceeds AL, diversion is indicated with confidence DP. The corresponding false alarm rate is FAP. The probability that, for a given alarm level, a diversion of magnitude B will not be detected is equal to 1 − DP: this is the nondetection probability (NDP) shown in Fig. 24.

For example, if the AL is set at 3σ, slightly more than one false alarm could be expected in 1000 material balance periods. Table X gives the probablity of detecting and failing to detect a diversion of magnitude B.

TABLE X

PROBABILITY OF DIVERSION DETECTION

Diversion Magnitude B	Detection Probability	Nondetection Probability
1σ	0.023	0.977
2σ	0.159	0.841
3σ	0.500	0.500
4σ	0.841	0.159
5σ	0.977	0.023
6σ	0.999	0.001

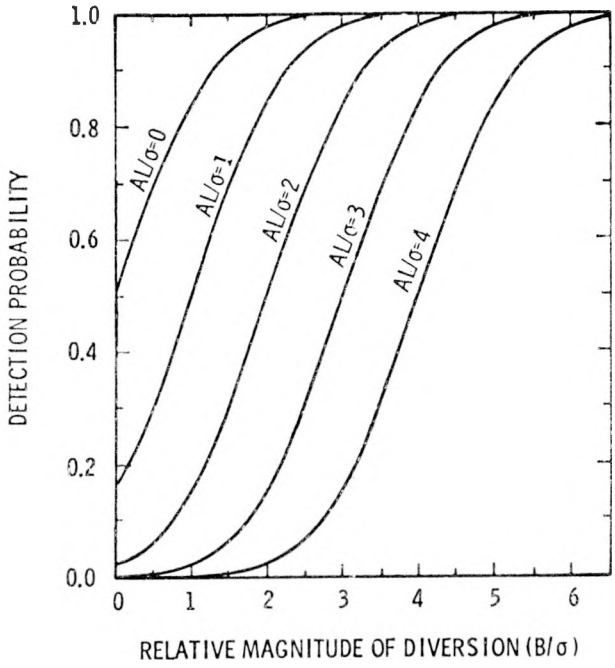

Fig. 22.
DP versus magnitude of diversion for several AL values.

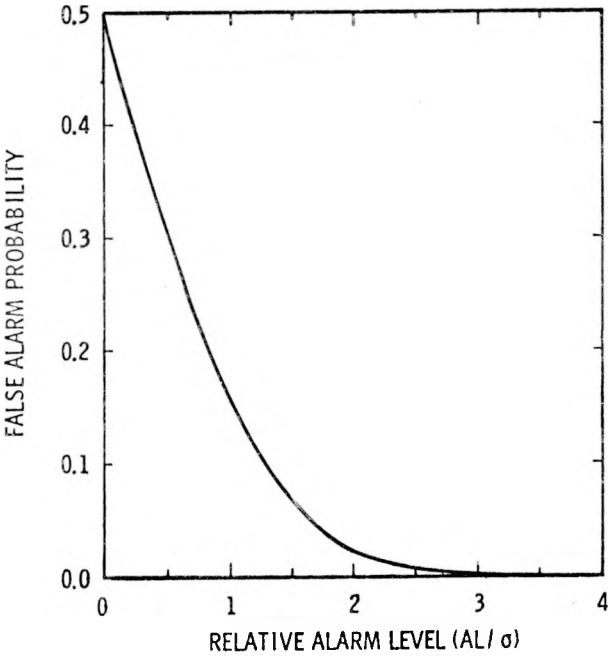

Fig. 23.
False alarm rate as a function of AL.

II. DYMAC IMPLEMENTATION

A. DP Site Test and Evaluation Phase

1. Ash-Leach Solution Assay System (R. S. Marshall, J. L. Parker, and R. Siebelist)

The plutonium solution measurement system previously described (Ref. 1, Sec. II-E, p. 8) was installed in the ash-leach glovebox array at DP Site, the present LASL plutonium processing facility. Figure 25 is a side cross-sectional view of the system.

Two unanticipated installation steps were necessary to reduce background count rates to acceptable levels. Removal of plutonium contamination from the inside glovebox floor immediately beneath the sample holder by wiping the surface with water-damp rags only reduced the surface contamination to approximately 2 g Pu/m² (0.2 g Pu/ft²). Subsequent scrubbing with an abrasive cleanser followed by washing with a 10% HCl solution further reduced the background by a factor of 20. The second unanticipated step was to decouple the GeLi detector lead shielding from the glovebox. Electronic or vibration-induced noise from the glovebox was eliminated by providing a 1-mm air gap between the lead shielding and the glovebox floor.

Initial calibration proceeded without difficulty and sample analyses were started. A program was set up with the LASL Analytical Chemistry Group CMB-1 to perform analyses on a large number of ash-leach liquid samples. The same samples will be assayed by the NDA solution assay system and a comparative statistical study will be made of the data.

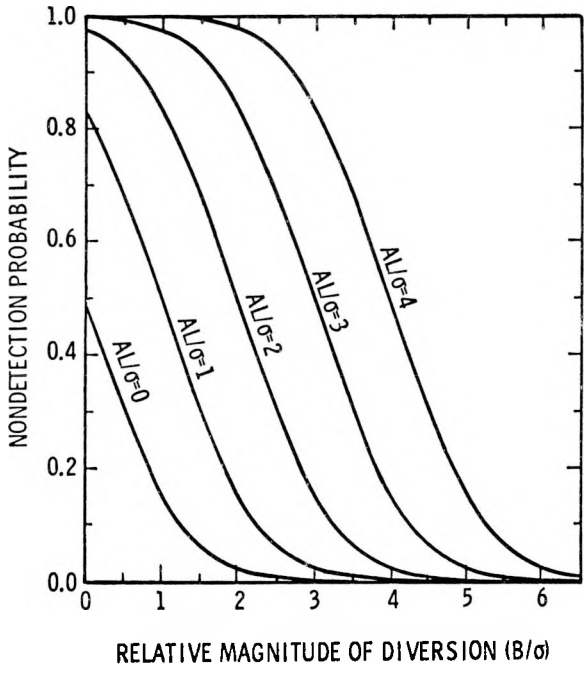

Fig. 24.
Probability of not detecting a diversion of magnitude B for several AL values.

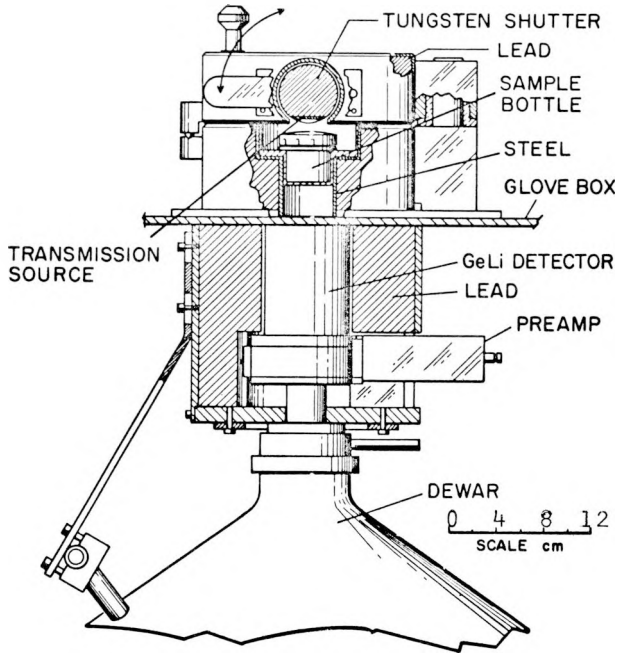

Fig. 25.
Plutonium solution measurement system.

2. In-Line Thermal Neutron Coincidence Counter (R. S. Marshall, N. Baron, and R. P. Wagner*)

The in-line thermal neutron coincidence counter (described previously in Ref. 1, Sec. IV-B-1b, p. 16) was fabricated. Electronic components were ordered and received and the system was assembled in Group R-1 laboratories. Preliminary testing was completed and the instrument performed to design specifications for both ^{240}Pu sensitivity and uniform response versus sample position.

Installation of the counter at DP Site and preliminary in-position checkout is expected to be completed during the May-August reporting period.

A number of plutonium standards are being prepared for the calibration of coincident neutron counters. They will contain PuO_2 of precisely measured plutonium content and isotopic composition. Matrixes of diatomaceous earth and MgO_2 will be used to simulate scrap materials processed at DP Site.

3. Computer Installation at DP Site (R. F. Ford**, J. Hagen, and C. Slocomb**)

The learning process and subsequent implementation of the existing nuclear material accounting system in conjunction with Group CMB-11 continues. A multiterminal program to emulate the current paper system was written and presented to CMB-11 for testing and evaluation. The group's suggestions are being incorporated into a revised version which will be tested during the next reporting period. The revised version will be used to operate a prototype four-terminal system in the recovery section of the DP Site operation. A deficiency in the current system introduces erroneous information entered by operators due to misread labels, transposition of digits, and the like. To overcome this deficiency, larger amounts of diagnostic tests have been added to the program to evaluate operator input.

The Nova 840 computer which is being used for the test and evaluation phase has been upgraded to 48 K words of memory. This allows us to test more of the features which will be needed in the new plutonium facility's system.

LASL Group CMB-11.
**LASL Group E-5.*

B. DYMAC for the New LASL Plutonium Facility (T. Gardiner, R. S. Marshall, R. F. Ford, J. Hagen, and C. A. Slocomb)

Numerous meetings have been held with Group CMB-11 personnel who are responsible for glovebox and equipment layouts in the new plutonium facility. These meetings produced a description of operations planned for each of the approximately 250 gloveboxes. Information such as SNM material type, quantity, containment, matrix, concentration, residence time, flow direction, waste generation, and physical or chemical processing steps has been documented. Blueprints show glovebox and conveyor line locations for the four separate areas within the new facility: ^{239}Pu R&D, ^{238}Pu R&D, metal fabrication, and recycle. Superposition of process information on the blueprints provides a basis for identifying NDA instrument and terminal locations, unit processes, unit process accountability areas (UPAAs), and MBAs.

Presently very specific and detailed information is being accumulated for each unit process which will be used for unit process modeling studies and for detailed design specifications of specific instruments. The detailed information is also being used to identify those areas where current instruments are inadequate. Instrument R&D efforts are, and will continue to be, directed to overcome deficiencies in current measurement methods and techniques.

III. TECHNOLOGY TRANSFER (R. H. Augustson)

Visits by managerial and technical staff continue to be the most frequent mode of communication. During this reporting period, 27 groups (a total of 55 persons) visited LASL for discussions with safeguards staff. They included representatives of NRC, ERDA, five foreign nations, the IAEA, and the nuclear industry.

REFERENCES

1. Nuclear Safeguards Research Program Status Report, September-December 1975, Los Alamos Scientific Laboratory report LA-6316-PR (April 1976).

2. R. H. Augustson and T. D. Reilly, "Fundamentals of Passive Nondestructive Assay of Fissionable Material," Los Alamos Scientific Laboratory report LA-5651-M (September 1974), p. 57.

3. C. D. Bingham, New Brunswick Laboratory, private communication to G. R. Keepin, October 1975.

4. Nuclear Analysis Research and Development Program Status Report, May-August 1974, Los Alamos Scientific Laboratory report LA-5771-PR (November 1974).

5. A. E. Evans and J. J. Malanify, "Nondestructive Assay of Inventory Verification Samples at the LASL Van de Graaff Small-Sample Assay Station," Nucl. Mater. Management **IV** (III), 309 (1975).

6. Nuclear Analysis Research and Development Program Status Report, January-April 1975, Los Alamos Scientific Laboratory report LA-6040-PR (August 1975).

7. Nuclear Analysis Research and Development Program Status Report, May-August 1973, Los Alamos Scientific Laboratory report LA-5431-PR (November 1973).

8. Nuclear Analysis Research and Development Program Status Report, September-December 1974, Los Alamos Scientific Laboratory report LA-5889-PR (April 1975).

9. D. F. Jones, L. R. Cowder, and E. R. Martin, "Computerized Low-Level Waste Assay System Operation Manual," Los Alamos Scientific Laboratory report LA-6202-M (February 1976).

10. E. Lopez-Menchero and A. J. Waligura, "The IAEA Programme for the Development of Safeguards Techniques and Instrumentation," Int. Symp. on the Safeguarding of Nuclear Materials, Vienna, October 20-24 (1975).

11. Nuclear Analysis Research and Development Program Status Report, May-August 1975, Los Alamos Scientific Laboratory report LA-6142-PR (December 1975).

12. R. Berg, G. Birkhoff, L. Bondar, G. Busca, J. Lev, and R. Swennen, "On the Determination of the ^{240}Pu in Solid Waste Containers by Spontaneous Fission Neutron Measurements, Application to Reprocessing Plant Waste," Eurochemic Technical report EUR-5158e (1974).

13. Nuclear Analysis Research and Development Program Status Report, September-December 1973, Los Alamos Scientific Laboratory report LA-5557-PR (February 1974).

14. L. V. East and R. B. Walton, "Polyethylene-Moderated ^{3}He Neutron Detectors," Nucl. Instrum. Meth. **72,** 161 (1969).

15. J. B. Marion and J. L. Fowler, "The ^{7}Li(p,n)^{7}Be Reaction," in *Fast Neutron Physics* (Interscience Publishers, Inc., New York, 1960), pp. 165-168.

16. C. Sonnier, Sandia Laboratories, private communication, 1976.

17. W. E. Gawthrop, Battelle-Columbus Laboratories, Progress Report BMI-X-699 (March 1976).

PUBLICATIONS

D. F. Jones, E. R. Martin, and L. R. Cowder, "Computerized Low-Level Waste Assay System Operation Manual," Los Alamos Scientific Laboratory report LA-6202-M (February 1976).

R. H. Augustson, T. D. Reilly, and T. R. Canada, "The LASL-U.S. ERDA Nondestructive Assay Training Program," J. Inst. Nucl. Mater. Management **V**(1) (1976).

H. O. Menlove, "Applications of ^{252} Cf in the Nuclear Industry," Intern. Symp. on Californium-252 Utilization, Paris, April 26-29, 1976.

GLOSSARY

AL	alarm level
BWR	boiling water reactor
DMA	direct memory access
DP	detection probability
DSS	Division of Safeguards and Security
DYMAC	DYnamic MAterials Control
ERDA	Energy Research and Development Administration
FAP	false alarm probability
HTGR	high-temperature gas-cooled reactor
IAEA	International Atomic Energy Agency
LASL	Los Alamos Scientific Laboratory
LED	light-emitting diode
LEMUF	limit of error of MUF
LWR	light-water reactor
MBA	material balance area
MUF	material unaccounted for
NBL	New Brunswick Laboratory
NDA	nondestructive assay
NDP	nondetection probability
NIM	nuclear instrument module
NRC	Nuclear Regulatory Commission
PROM	programmable read-only memory
PWR	pressurized water reactor
RAM	random access memory
SAM	stabilized assay meter
SCA	signal-channel analyzer
SNAP	shielded neutron assay probe
SNM	special nuclear material
SSAS	small sample assay station
UPAA	unit process accountability area
USAD	uranium solution assay device

☆ U.S. GOVERNMENT PRINTING OFFICE: 1976—777-018/4